Title

tRNA Genes Affect Chromosome Structure and Function via Local Effects

Journal

Molecular and Cellular Biology, 39(8)

ISSN

0270-7306

Authors

Hamdani, Omar
Dhillon, Namrita
Hsieh, Tsung-Han S
et al.

Publication Date

2019-04-01

DOI

10.1128/mcb.00432-18

Peer reviewed

Transfer RNA Genes Affect Chromosome Structure and Function via Local Effects

Omar Hamdani[1*], Namrita Dhillon[1*], Tsung-Han S. Hsieh[3*], Takahiro Fujita[4*], Josefina Ocampo[5*], Jacob G. Kirkland[1], Josh Lawrimore[6], Tetsuya J. Kobayashi[7], Brandon Friedman[6], Derek Fulton[6], Kenneth Y. Wu[1], Răzvan V. Chereji[5], Masaya Oki[4], Kerry Bloom[6], David J Clark[5], Oliver J. Rando[3], Rohinton T. Kamakaka[1,2]

1 Department of MCD Biology**,** 1156 High Street, University of California, Santa Cruz, CA 95064 USA
E-mail: rohinton@ucsc.edu
2 Corresponding Author
3 Department of Biochemistry and Molecular Pharmacology, University of Massachusetts Medical School, Worcester, MA 01605, USA
4 Department of Applied Chemistry Biotechnology, University of Fukui, Bunkyo, Fukui, Japan.
5 Division of Developmental Biology, Eunice Kennedy Shriver National Institute of Child Health and Human Development, 6 Center Drive, Bethesda MD 20892 USA
6 Department of Biology, University of North Carolina at Chapel Hill, Chapel Hill, NC 27599-3280 USA
7 Institute of Industrial Science, The University of Tokyo, Tokyo, Japan

* These authors contributed equally

Abstract

The genome is packaged and organized in an ordered, non-random manner and specific chromatin segments contact nuclear substructures to mediate this organization. Transfer RNA genes (tDNAs) are binding sites for transcription factors and architectural proteins and are thought to play an important role in the organization of the genome. In this study, we investigate the role of tDNAs in genomic organization and chromosome function by editing a chromosome so that it lacks any tDNAs. Surprisingly our analyses of this tDNA-less chromosome show that loss of tDNAs does not grossly affect chromatin architecture or chromosome tethering and mobility. However, loss of tDNAs affects local nucleosome positioning and the binding of SMC proteins at these loci. The absence of tDNAs also leads to changes in centromere clustering and a reduction in the frequency of long-range *HML-HMR* heterochromatin clustering with concomitant effects on gene silencing. We propose that the tDNAs primarily affect local chromatin structure that result in effects on long-range chromosome architecture.

Introduction

The three dimensional organization of the yeast nucleus is non-random (Reviewed in [1, 2]). Each chromosome occupies a specific territory in the nucleus anchored to nuclear substructures via specific DNA sequences. The telomeres of each chromosome tend to associate with one another and with the nuclear envelope in small clusters, based on the length of the chromosome arms [3-5]. The rDNA repeats on chromosome XII are packaged into a dense structure known as the nucleolus, which also localizes to the nuclear periphery [6]. Opposite the nucleolus is the spindle pole body, which is the interphase attachment site for the centromeres of the 16 chromosomes [7]. Attachment of centromeres to the spindle pole and attachment of telomeres to the nuclear membrane dependent upon chromosome arm length helps organize the nucleus [8]. The active genes along the chromosome arms primarily reside in the nuclear interior though some active genes including some tRNA genes interact with nuclear pores and help tether the arms [1, 9, 10].

Besides DNA sequence elements, numerous proteins play a role in nuclear organization via networks of interactions between nuclear membrane and chromatin bound proteins. Chromatin bound proteins involved in this organization include heterochromatin proteins, [11], lamin like proteins [12-16], specific transcription factors [17, 18], RNA polymerases [6] and DNA repair proteins [19, 20] (see [1] for review).

tRNA genes (tDNAs) are a class of active genes found on all chromosomes and are bound by transcription factors TFIIIB and TFIIIC and RNA polymerase III. tDNAs are short, highly transcribed DNA sequences [21] that are usually nucleosome-free with strongly positioned flanking nucleosomes [22-25]. The tDNAs contain internal promoter

elements called A and B-boxes, which aid in the binding of the transcription factor TFIIIC [26, 27]. TFIIIC helps recruit TFIIIB to AT rich sequences upstream of the tDNA. tDNA-bound transcription factors function via interactions with cofactors. tRNA genes are sites of binding for numerous chromatin proteins including the architectural SMC proteins, nuclear pore proteins, chromatin remodelers and histone modifiers. Studies from several labs have shown that tDNAs are enriched in cohesin (Smc1/Smc3) [28], and condensin (Smc2/Smc4) complexes [29, 30], as well as the SMC loading proteins (Scc2/Scc4) [31, 32] and some chromatin remodelers including RSC [22, 29, 33-35].

While individual tRNA genes turn over rapidly as a result of mutational inactivation and gene loss [36-38], a subset of tDNA are syntenic with respect to neighboring sequences [39, 40] and data suggest that these conserved tDNAs possess chromosome position-specific functions in gene regulation (reviewed in [41, 42]). There are several position-specific effects mediated by tDNAs. First, tDNAs have been shown to function as heterochromatin barrier insulators, which stop the spread of heterochromatic domains into adjacent non-silenced domains [35, 39, 43, 44]. Second, tDNAs block communication between enhancers and promoters when located between these elements in yeast, *Drosophila*, mouse and human cells by acting as enhancer blockers [39, 45-50]. Third, the presence of a tDNA in close proximity to a RNA pol II transcribed gene promoter antagonizes transcription from the pol II transcribed gene in a phenomenon refereed to as tRNA gene mediated silencing (tgm silencing) [30, 51, 52].

In many organisms, tDNAs have also been shown to cluster at sites in the nucleus [39, 42, 53-55]. In *S. cerevisiae*, DNA FISH studies have shown that some tDNAs

cluster together adjacent to centromeres [52, 54] while proximity ligation analysis suggest that tDNAs cluster at the outer periphery of the nucleolus as well as near the centromeres [10] though more recent HiC studies seem unable to detect these long-range associations [56]. Based on these results it has been proposed that TFIIIC binding to discrete sites along the chromosome plays an important role in chromosome folding and organization in the yeast nucleus [54, 57, 58].

To better analyze the role of tDNAs in chromatin looping and organization we generated a “tDNA-less” chromosome through the systematic deletion of all the tDNAs on chromosome III in *S. cerevisiae*. We characterized chromatin packaging, chromosome folding and nuclear dynamics of this chromosome. We show that tDNA loss affects nucleosome positioning and loading of SMC proteins in the vicinity of tDNAs but this has no effect on chromatin looping. While loss of the tDNAs does not affect chromatin looping, it does affect centromere clustering and the long-range interactions of the silenced *HML* and *HMR* loci with concomitant effects on gene silencing.

Results

The ~275 tDNAs in the budding yeast genome are dispersed across all 16 chromosomes. Here, we focus on chromosome III, which is 316 kb long and has two tDNAs on the left arm and eight tDNAs on the right arm. In order to investigate the role of tDNAs in chromatin looping, nuclear organization and function, we created a strain in which chromosome III is devoid of any functional tDNAs by deleting an internal fragment of each tDNA. The deletions eliminate the internal promoter elements (both BoxA and BoxB) and thus eliminate the binding of the transcription factors TFIIIC and TFIIIB. For simplicity, we have labeled the tDNA adjacent to the *HMR* locus as t0 and have labeled the remaining nine tDNAs going from right to left as t1, t2, t3 etc. To delete the tDNAs we first replaced an internal segment of the gene with a *URA3* gene and then subsequently replaced *URA3* with a DNA fragment containing a unique DNA barcode. This involved multiple sequential transformations. Each deletion was monitored by PCR analysis, and intermediate strains were backcrossed to wild type W-303 prior to additional rounds of transformations. All of the experiments described were performed in this strain background to avoid strain specific effects.

Most tRNA isoacceptor families have multiple copies, scattered throughout the genome, though single gene copies code for six isoacceptor families. On chromosome III eight of the ten tDNAs that were deleted are members of multi-copy gene families (with 10-16 copies in the genome) and are not essential. However, tDNA t1 (*tS(CGA)c*) is a single copy gene and is essential in *S. cerevisiae* [59] and there are only two copies of tDNA t7 (*tP(AGG)c*) in the genome. Loss of t7 from chromosome III caused cells to grow more slowly. In order to remove these two genes from chromosome III and

simultaneously maintain the health of the yeast, we integrated single copies of these two genes on chromosome XV at the *HIS3* locus. Once the full tDNA deletion chromosome III had been constructed, the strain harboring this chromosome was backcrossed with wild-type W-303, and segregation of the deleted tDNAs was monitored by PCR using primers specific to the unique barcodes. The sequence of this modified chromosome is available.

The strain where chromosome III lacked any tDNAs (tDNA delete) was grown in rich media at 30C and did not show any obvious growth defect, forming homogeneous and healthy, smooth edged colonies. Strains bearing this tDNA-less chromosome had a doubling time of ~90 minutes in liquid YPD media, which was indistinguishable from a wild type strain. This is consistent with data showing that loss of one copy of multi-copy tDNAs in yeast cells do not lead to growth defects in rich media [60].

We analyzed the wild type and tDNA mutant strain for sensitivity to various stresses. We grew haploid cells on plates containing increasing concentrations of hydroxyurea, benomyl and caffeine. This analysis showed that the tDNA delete strain was as resistant to these drugs as the wild type cells (Figure 1).

Changes to the local nucleosome landscape surrounding the tDNAs

The stable binding of TFIIIC and TFIIIB as well as their interactions with chromatin remodelers result in nucleosome eviction at the tDNA and positioning of nucleosomes adjacent to the gene [22, 61]. At some tRNA genes a single nucleosome appears to be disrupted while at other tDNAs multiple nucleosomes are disrupted. Since tDNAs are dispersed across the chromosome and are highly transcribed, we first asked if loss of all ten tDNAs from the chromosome altered the nucleosome and transcription landscape of

the chromosome. In order to determine if tDNAs affect nucleosome positions across chromosome III, we mapped nucleosomes in our tDNA delete strain as well as in the wild type strain.

Haploid yeast cells were grown to log phase, harvested and nuclei were digested with varying concentrations of micrococcal nuclease to generate mono-nucleosome protected DNAs, which were subjected to paired-end MNase-seq. Overall, the nucleosome landscape across all chromosomes except chromosome III was unaffected by the presence or absence of the chromosome III tDNAs. More focused analysis showed no change in nucleosome positioning in the proximity of the 265 tDNAs scattered on the 15 chromosomes that were not manipulated in this study (Figure 2A).

In contrast, changes in nucleosome occupancy were observed at or immediately adjacent to the deleted tDNAs on chromosome III. Figure 2B shows the average nucleosome occupancy across 2kb segments centered on the chromosome III tDNAs with each tDNA in WT cells aligned at its 5' end while in the tDNA delete strain, the 5' ends of the deletion points were aligned. In the wild type strain there is a clear nucleosome free region centered on the tDNA flanked by positioned nucleosomes reflecting differential digestion of the TFIIIB-TFIIIC complex relative to nucleosomes [35, 62]. In the tDNA delete strain this pattern is altered and a nucleosome is usually formed over the deletion junction (see Figure2D). We were unable to determine the change in the chromatin landscape around t1 and t7 tDNAs since these two genes with 100 bp of flanking sequences were transposed to the *HIS3* locus. Nucleosome positions elsewhere on chromosome III that are distant from the tDNAs are not altered on the tDNA-less chromosome (Figure 2C). These results demonstrate that tDNAs create

nucleosome free regions at the tRNA gene with positioned nucleosomes flanking the gene. The data also show that their chromatin organizing effects are locally confined and do not extend beyond their immediate vicinity.

tDNA loss affects expression of few RNA pol II transcribed genes

The presence of a tDNA in close proximity to a RNA pol II transcribed gene promoter antagonizes transcription from the pol II transcribed gene called tRNA gene mediated silencing (tgm silencing) [30, 51, 52]. In addition, tDNAs have also been shown to function as enhancer blockers when located between an UAS enhancer and a promoter [47]. Since the loss of the tDNAs altered nucleosomes in their vicinity we wondered if these alterations affected the transcription landscape of genes on chromosome III. Rather than restrict the analysis to pol II transcribed genes adjacent to the tDNAs on chromosome III, we investigated the effects of tDNA loss on all pol II transcribed genes in the genome and analyzed the changes in RNA levels in the wild type and tDNA delete strain by RNA-seq. Total RNA was extracted from exponentially growing yeast cultures and RNA-seq libraries were prepared, sequenced and analyzed as described in the materials and methods section. The RNA levels of a very small number of genes were affected upon deletion of the tDNAs. Table1 lists the genes that were either up regulated or down regulated in the strain lacking tDNAs on chromosome III. Of the ten tDNAs present on chromosome III, tDNA t0, t8 and t9 are flanked by retrotransposon elements and since these are repetitive elements, the tDNA-mediated transcription effects could not be investigated for these loci. Furthermore, tDNAs t3 and t4 are missing in W-303. The expression of only two genes on chromosome III was affected and in both instances, a tDNA (t1 and t6) was located adjacent to the gene. In one

instance the gene was up regulated upon tDNA loss while in the second instance the gene was down regulated. Furthermore, we observed the up regulation of the *MRM1* gene. This gene resides immediately adjacent to *HIS3*. The tDNAs for t1 and t7 were ectopically inserted at the *HIS3* locus in the tDNA delete strain demonstrating that the ectopic insertion of the tDNAs is the cause of the change in expression of *MRM1*. These data suggest that tDNA mediated position effects are highly context dependent and only affect some pol II transcribed genes and not others.

Of the genes that were down regulated in the tDNA delete strain, several are involved in amino acid biosynthesis though these genes are scattered throughout the genome and do not localize near tDNAs. The reason why expression of these genes was reduced is unclear given that the two yeast strains used are isogenic with respect to nutritional markers, and there are between 10 and 16 copies of each of the six deleted tDNAs in the genome (t0=11 copies, t2=10 copies, t5=16 copies, t6=11 copies, t8=10 copies and t9=15 copies). It is possible that there is a reduction in transcript levels of these genes due to the small reduction in tDNA copy number without any other cell phenotype. This is consistent with a recent study where single tDNAs in yeast were deleted and these single deletions in multi-copy tDNA families also led to changes in the expression of a small set of genes involved in translation [60].

Scc2 binding at tDNAs is dependent upon a functional tDNA but other binding sites are tDNA independent

The SMC proteins play an important role in nuclear organization [63] and tDNAs are major binding sites for SMC proteins and the SMC loaders Scc2/Scc4 and Rsc. Our nucleosome mapping data indicated that loss of the tDNAs altered nucleosome

positions at tDNAs. Since nucleosome free tDNAs are sites for the recruitment of RSC and Scc2/Scc4 proteins [31, 34, 64, 65], we asked if loss of all the tDNAs on chromosome III reduced recruitment of Scc2 proteins at these loci and whether it also affected loading of Scc2 at other sites along the chromosome.

We performed a ChIP-seq of Myc-tagged Scc2 to compare the distribution of this protein genome wide in the WT and tDNA delete strain (Figure 3). This analysis showed Scc2 binding at multiple sites along the chromosome including tDNAs. At some tDNAs the Scc2 binding is focused forming a sharp peak while at other tDNAs the binding is spread over a greater region. Comparison between the wild type and tDNA delete strain showed that Scc2 levels did not decrease at any of the sites on the 15 chromosomes. Upon tDNA loss Scc2 binding decreased at the tDNA loci on chromosome III or at sites in the immediate vicinity of tDNAs such as *LEU2* (adjacent to tDNA t8) (Figure 3) and *HMR* (adjacent to t0). On chromosome III the analysis also showed that there was no significant change in Scc2 binding at other non-tDNA sites on chromosome III. For example we saw a large peak of Scc2 binding at Tel3L. This peak at Tel3L was unchanged upon tDNA deletion and similarly we did not record any change in Scc2 levels at *CEN3* confirming that tDNAs are not the sole determinants for the recruitment of Scc2 to chromosomes.

We confirmed this result by ChIP-qPCR against Scc2. A site at the *OCA4* gene was used as an internal control since this site does not bind Scc2 in wild type cells. We were unable to design unique primers at t6 due to the presence of repetitive sequences in the immediate vicinity of this gene and therefore could not map the localization of these proteins at this tDNA. Some primer pairs flank the tDNAs while others are adjacent to

246 the tDNAs. Consistent with the ChIP-Seq data, in wild type cells, Scc2 is enriched at
247 several of the tDNAs present on chromosome III (Figure 4A). We observed ~3.5 fold
248 enrichment at t8 and ~2.5 enrichment at t0, t2 and t5. When the same protein was
249 mapped in the tDNA delete strain we observed a significant reduction in Scc2 binding at
250 these tDNAs. The levels dropped to those observed for the negative control *OCA4*
251 except for the t8 tDNA, where the level dropped two fold but there was some residual
252 Scc2 still present (Figure 4A). The amount of Scc2 did not change at *CEN3* when the
253 tDNAs were absent from the chromosome, indicating that the binding of Scc2 to the
254 centromere was independent of the tDNAs.
255 Scc2, in association with Scc4 helps recruit the SMC proteins to chromatin [29, 32].
256 Condensins localize to tDNAs and are necessary for the clustering of tDNAs in the
257 nucleus [29, 30]. We therefore mapped the binding of condensins at tDNAs on
258 chromosome III using the HA-tagged Brn1 subunit. In wild type cells, the Brn1 profile
259 was very similar to that previously observed for Scc2 with significant binding of Brn1 at
260 specific tDNAs. Correspondingly, the binding of the condensins was significantly
261 reduced at these sites upon deletion of the tDNA promoters (Figure 4B).
262 **Chromosome mobility on the tDNA-less chromosome**
263 TFIIIC binding sites and tDNAs are described as chromosome organizing clamps
264 because of their consistent association with specific landmarks within the nucleus [54].
265 The localization of tDNAs with the kinetochore is dependent upon condensins while the
266 interactions of tDNAs with nuclear pores in the G2 phase of the cell cycle are dependent
267 upon cohesins. These associations likely help tether the chromosome. Since loss of
268 tDNAs from chromosome III led to a decrease in SMC proteins from these sites we

wondered if this loss would affect chromosome tethering and mobility of the chromosome. To assess mobility we fluorescently-labeled specific sites on chromosome III, and used these to monitor chromosome mobility in the wild type and the tDNA deletion chromosomes. The location of a point on the chromosome was mapped in three-dimensional space over a defined period of time in relation to another point within the nucleus- the spindle pole body (marked with the Spc29-RFP fusion protein)- and mobility was characterized by mean square distance analysis (MSD) as described previously [66-68]. Six chromosomal loci across chromosome III were assayed (Figure 5). These loci were tagged by inserting LacO arrays at these sites and monitored using a LacI-GFP fusion protein mediated fluorescence. Time-lapse movies of >35 individual unbudded cells (in the G1 phase of the cell cycle) were imaged over the course of 10 minutes. Z-stack images of the cells were taken every 30 seconds during the time-lapse, and MSD was calculated at each time-point using the following equation: $<(X_t - X_{t+\Delta t})^2>$. Using this information, MSD curves were generated for each locus in both the WT and tDNA delete strain (data not shown). For the wild type chromosome III, *CEN3* was the most constrained locus (Rc=415 nm), with loci located further from the centromere exhibiting greater mobility. For example, *LEU2*, which is approximately 30kb from the centromere, had an Rc of 522nm while *HMR*, which is approximately 180kb from the centromere, had an Rc value of 688nm. This is consistent with previous data showing that the location of a locus in relation to the centromere is critical in determining its mobility, with loci closer to the centromere displaying decreased mobility compared to loci farther from the centromere [9, 68, 69]. Comparison of mobility of segments in the wild type and tDNA delete strains, showed a small decrease in mobility in the tDNA

delete strain at a couple of sites (*SRO9* and *CEN3*). However these differences were not statistically significant (p values= 0.15 and 0.19). The data indicate that tDNAs are not major determinants in constraining chromosome arm motion or that they are a subset of factors involved and the redundancy precludes observation of their contribution.

tDNAs are not required for proper chromatin folding

Transfer RNA genes have been proposed to affect chromatin fiber folding via the clustering of dispersed tRNA genes. The promoters in tDNAs are the binding site for the transcription factor TFIIIC and foci comprised of multiple TFIIIC-bound sites have been proposed to function in chromatin looping and folding [10, 39, 52-54, 57, 58, 70]. If tDNAs are major drivers of chromatin folding and looping, then elimination of these loci from an entire chromosome should lead to changes in the folding of the chromatin fiber or result in changes in chromosome packaging in the nucleus. We set out to determine the detailed three-dimensional organization of chromosome III lacking functional tDNAs. We used a modified chromosome conformation capture technique called Micro-C XL [71, 72]. We chose Micro-C XL over HiC because it can capture both short length 3D interactions as well as some long-length interactions and the method is not dependent upon the distribution of restriction sites along the DNA. In brief, yeast cells were first cross-linked with formaldehyde and DSG, and chromatin was then fragmented into mono-nucleosomes via micrococcal nuclease digestion. Cross-linked, digested chromatin was ligated to capture chromosomal interactions. Size-selected ligation products were then purified and subjected to paired-end high-throughput sequencing. Sequencing reads were mapped back to the reference genome to determine the

interacting regions of the chromosome, as previously described. For each strain two independent cross-linking and ligations were performed and QuASAR (Quality Assessment of Spatial Arrangement Reproducibility) and Genome DISCO (Differences between smoothed contact maps) were used to assess the reproducibility of the data. The two independent measurements both gave a score >95% confirming the reproducibility between the two biological replicates for the wild type and tDNA delete strain. Reproducibility of the data was also analyzed by measuring contact probability over genomic distance and the decay curves between replicates overlapped almost completely which is consistent with our reproducibility measurements.

Overall, Micro-C maps for wild type and tDNA mutant strains both exhibited previously described features of yeast chromosome folding, with no difference in chromatin folding between the tDNA delete and wild type strains. The chromatin interaction maps of chromosome IX show that most Micro-C interactions occurred close to the diagonal in both strains though there was significant variation in the density along the diagonal. The data clearly show ~2-10kb contact domains (CIDs/TADs) encompassing ~1-5 genes in both strains (Figure 6A). We calculated the insulation score across bins and a scatter plot of the insulation scores for wild type and mutant strains is consistent with the conclusions that the overall architecture of chromosomes in these two strains was not altered (Figure 6B).

Inspection of the chromosome III in the wild type and tDNA delete cells showed that these interaction domains persisted on this chromosome even upon loss of the tDNAs from chromosome III. The interaction decay curve for chromosome III is very similar in the wild type and tDNA delete strain indicating that the overall folding of the

chromosome has not altered (Figure 6C). There was no significant change in the contact frequency versus genomic distance in the two strains, indicating no local chromatin decondensation or change in chromatin looping interactions.

We analyzed the contact frequency of sites immediately adjacent to the 8 tDNAs on chromosome III in the wild type and tDNA delete strains. At some sites, the loss of the adjacent tDNA did not alter long-range interactions at all while at other sites there was small changes though the significance of these remains to be elucidated (Figure 6D).

Thus, tDNAs do not appear to be responsible for the general folding of the chromatin fiber and the CID/TAD architecture.

tDNAs affect CEN-CEN interaction frequency

While the overall folding of the chromatin fiber of chromosome III was not altered micro-C analysis identified changes in contact frequency at specific sites along chromosome III. In order to identify sites where contact frequency had changed the contact maps were normalized by distance for the wild type and tDNA delete strains (Figure 7A). These matrixes were used to identify differential contact sites (generated by dividing the tDNA delete matrix by the wild type matrix). This analysis identified increased sites of contacts in the tDNA delete strain (shown in red) around the centromere and near the telomeres of chromosome III (Figure 7B).

The 16 centromeres in yeast are in close physical proximity to one another and cluster adjacent to the spindle pole body [7, 73, 74]. These CEN-CEN interactions are readily captured by 3C methods including HiC [10, 71, 75], and are recapitulated in this study in the W-303 strain background. Interestingly compared to the wild type strain, the centromere of chromosome III in the tDNA delete strain showed an increased frequency

of interactions with the other centromeres. Focusing on the 50kb pericentric region of each chromosome, we found that most CEN-CEN interactions were minimally affected by the loss of chromosome III tDNAs. For instance, interactions between the chromosome XVI centromere and the remaining centromeres showed that interactions between *CEN16* with the majority of centromeres remained unchanged, but that there was a ~20% increase in interaction strength between *CEN16* and *CEN3* when chromosome III lacked tDNAs (Figure 7C).

This increase in *CEN3* interaction was not confined to *CEN16*. When the same analysis was performed using *CEN3* as an anchor, we observed increased frequency of interactions between *CEN3* and all of the other chromosomal centromeres in the tDNA delete strain (Figure 7D). Most of the interaction counts increased approximately 20% compared to WT, with the highest increase seen at C*EN3-CEN9*. The increase in the CEN3-CEN interactions in the tDNA deletion strain was significantly higher ($p=1.22x10^{-14}$) compared to values of all CEN16-CEN interactions (excluding CEN16-CEN3). These results show that upon deletion of all tDNAs across chromosome III, inter-chromosomal interactions increase between *CEN3* and the other centromeres, suggesting that functional tDNAs likely antagonize CEN-CEN associations during interphase.

We next measured chromosome loss rates of wild type and tDNA delete diploid cells. We first constructed homozygous diploid cells containing *URA3*, *TRP1* and the *MAT* locus located on chromosome III (in both the wild type and tDNA delete strain). Single diploid colonies were grown for 20 doublings in YPD and approximately 10^7 cells were plated onto 5-FOA plates to measure the number of cells that had become *URA3* negative. Cells could have become uracil auxotrophs by gene mutations or via loss of

the chromosome. These two types of mutants could be distinguished by replica plating the 5-FOA resistant colonies onto plates lacking tryptophan or by checking for the appearance of MATα pseudo haploid cells. The number of cells unable to grow on media lacking trypthophan and also being able to mate were counted and chromosome loss rates were calculated by dividing the number of these colonies by the total number of cells plated. In wild type cells the loss rate for chromosome III was 4.08×10^{-5} and is in agreement with previous reports [76]. The loss rates for the tDNA delete chromosome decreased slightly to 3.26×10^{-5} suggesting that loss of the tDNA slightly helped stabilize the chromosome ($p=0.02$).

tDNAs play a role in *HML-HMR* long-range association

The silent loci *HML* and *HMR* reside on chromosome III separated by approximately 300kb along the linear chromosome. However, the *HML* locus, located 11kb from *TEL3L*, is in close three-dimensional proximity to the *HMR* locus, located 23kb from *TEL3R*. This long-range interaction has previously been detected using both live-cell microscopy and HiC analysis [20, 75, 77] and we recapitulate this finding in the Micro-C experiment with the wild type strain (Figure 8A). Comparing wild type cells to the tDNA delete strain, we noticed that the interaction of *HML* with *HMR* was slightly altered in the tDNA delete strain. In wild type cells, there was an interaction between *HML* and *HMR* and this interaction zone became less defined and more diffuse upon deletion of the tDNAs and a slightly increased interaction frequency was observed across a broader region of the end of chromosome III. While *HMR* still interacted with *HML* in the deletion strain, it appeared to also display interactions with other loci (including *TEL3L)*. Similarly, the segment containing *HML/TEL3L* showed increased interactions with

TEL3R rather than being restricted to interacting with sequences at *HMR*. These results suggest that deletion of chromosome III tDNAs subtly perturbed *HML-HMR* long-range interactions.

Given that Micro-C measures population averages of stable long-range interactions we decided to measure *HML-HMR* interactions in live cells using fluorescence microscopy. We wished to determine if the tDNAs influenced *HML-HMR* interactions. We generated a strain with multiple Lac operator sequences inserted adjacent to *HMR* (at the *GIT1* gene) and multiple copies of the Tet operator sequences inserted adjacent to *HML.* Expression of the fusion proteins CFP-LacI and YFP-TetR in this strain enabled us to visualize these loci in living yeast by fluorescence imaging. The distance between *HML* and *HMR* was then measured in wild type and a strain lacking the t0 tDNA (Figure 8B). We found that in wild type cells, *HML* was in close proximity to *HMR*. Consistent with our expectations, deletion of Sir proteins resulted in separation of these loci validating this assay. Importantly, when we eliminated the t0 tDNA, this led to a change in the distance between *HML* and *HMR* compared to wild type cells, with the median distance between *HML* and *HMR* increasing upon deletion of the tDNA. Given the presence of outliers in the data we used a Mann-Whitney U-Test to determine statistical significance between wild type and the mutant. With an n of approximately 300 cells for the wild type and tDNA delete strain we observed a p value of $3.1\ e^{-14}$ showing that the differences observed between the two strains were significant. Closer analysis of the plot indicates that upon deletion of the tDNA there is heterogeneity in the distances between the two loci and a continuum of values. Thus there are cells where the two loci are in very close proximity as well as cells where the two loci are further apart. It should

be noted that the HiC approach and the microscopic method to measure proximity are inherently different and distinct and each method provides different types of information and each approach has specific limitations. Use of long arrays bound tightly by repressor proteins that dimerize may influence chromatin architecture and fluorescence measurements [78]. Similarly the HiC based methods are influenced by indirect crosslinking especially in regions of condensed heterochromatin and nuclear substructures like sites near centromeres and the nuclear envelope [79-81].

The tDNA t0 is necessary for the recruitment of cohesins to the silenced loci and the SMC proteins are necessary for long-range *HML-HMR* interactions [20]. However not all tDNAs are equivalent in their ability to recruit cohesins to the silenced loci [43, 82, 83]. We therefore inquired if tDNAs that are unable to recruit cohesins are able to restore long-range association between *HML* and *HMR*. We replaced the *HMR* $tDNA^{THR}$ (t0) with $tDNA^{THR}$ (NL1) from chromosome XIV. This tDNA has identical sequence to the t0 tDNA in the body of the gene and therefore has the identical BoxA and BoxB promoter sequence and spacing as tDNA t0. However sequences flanking this tDNA are distinct and the NL1 tDNA is unable to recruit/bind cohesins [82, 83]. The NL1 tDNA has reduced binding of TFIIIC and a narrower nucleosome free region as well [62, 84]. This tDNA also has reduced nucleoporin binding and reduced histone turnover frequency [61, 85]. When we replaced a 300bp t0 tDNA-containing fragment with a 300 bp NL1 tDNA-containing fragment we found that the NL1 tDNA was not able to robustly restore long-range *HML-HMR* interactions, suggesting that tDNA mediated local chromatin organization might be necessary for these long-range interactions.

Replication fork pausing at tDNA mediates long-range chromosomal interactions

We had previously shown that DNA double strand repair proteins help deposit cohesins to the silenced loci, which then lead to homology dependent long-range interactions between *HML* and *HMR* [19, 20]. Since we had discovered that a specific tDNA helped in the clustering of *HML* and *HMR*, we wished to know the mechanism by which this phenomenon occurred. Replication fork pausing/stalling is observed at many tDNAs. This results in the deposition of γ-H2A at the tDNA and this is necessary for fork recovery from the pause/stall [20, 29, 86-90]. Rrm3 and topoisomerases play a role in the recovery of stalled replication forks at protein bound sites in the genome such as tDNAs [88, 91, 92]. Therefore we analyzed the effect of these mutants on *HML-HMR* long-range association. The data show that deletion of Rrm3 as well as mutants in the DNA polymerase-ε subunit Dpb3 and the topoisomerase Top1 lead to a statistically significant decrease in *HML-HMR* long-range association (Figure 5B and figure legend). Thus the presence of a tDNA as well as normal Rrm3, Top1 and Dpb3 function are necessary for the establishment or maintenance of the long-range association between *HML* and *HMR*.

tDNA enhances epigenetic gene silencing at clustered *HML-HMR*

Since the tDNA is necessary for the long-range clustering of the silenced domain, we wondered if reduction in clustering had any effect on gene silencing. We asked whether tDNA mediated loss of *HML-HMR* interactions affected gene silencing at *HML* and *HMR*. Silencing can be assayed by insertion of reporter genes within or immediately adjacent to the silenced domains. In wild type yeast when a reporter gene

is inserted immediately adjacent to these loci, the gene is metastably silenced. A cassette containing an H2B (*HTB1*) promoter driving *HTB1-EYFP* was integrated to the right of *HML* while a cassette containing the *HTB1* promoter driving *HTB1-ECFP* was integrated to the left of *HMR*. In addition, on chromosome XV, a cassette containing an *HTB1*promoter driving *HTB1*-mCherry was integrated as a control euchromatic marker [93]. The *HTB1*-mCherry gene is active in all cells in the population. The *HML::YFP* and the *HMR::CFP* reporter genes are present immediately outside of *HML* and *HMR* but reside in a region bound by Sir proteins [4, 22]. These genes adopt one of two expression states, either active or silent. For visualization, single cells were placed on microfluidic plates and monitored continuously by fluorescence microscopy. Fluorescent signal from each individual cell was recorded every 40 minutes over a period of ~24 hours. This allowed us to trace the lineage of each daughter from the founder cell and score the cells according to the expression of the reporter genes at *HML* and *HMR*. Cell lineage trees were traced and each cell in the lineage was assigned a positive or negative value for expressing each reporter as it underwent cell division (Figure 9A).

We initially analyzed the silencing of the reporter genes in the wild type strain. Consistent with previous data [93], reporters at *HML* and *HMR* were regulated such that the reporters maintained their activity state over many generations and occasionally switched to the opposite expression state. Once they switched they maintained the new state for several generations. Furthermore, when one reporter was active the other was also more likely to be active suggesting long-range coordination between *HML* and *HMR* though this coordination is not absolute.

We next investigated silencing of the reporters in a strain where chromosome III lacked all the tDNAs. In this strain, the reporter at *HMR* was active more often compared to the wild type strain. While the effect was not as pronounced, the same effect was also observed at *HML* (Figure 9A tDNA delete panel). Furthermore, the silenced state was less stable, and switched to the active state more often. This suggests that silencing at these loci is influenced by the tDNAs.

While expression states at both *HML* and *HMR* were stably inherited, the transcriptional state did flip in daughter cells (Figure 9B). An expressed to repressed transition was a less frequent event compared to the repressed to expressed transitions regardless of genotype. This is not entirely surprising since the reporter genes were inserted immediately outside of the two silencers in a zone where the silent state is metastable [94, 95]. However, when analyzing the repressed to expressed transitions, we saw a discernible difference in the frequency of the expression of the reporter genes at *HMR*. The full tDNA delete strain showed an increased frequency of cells undergoing the transitions at *HMR* compared to wild type cells and the inverse was seen for the expressed to repressed transition (Table 4).

Given that the transcription states of the reporters were affected at both *HML* and *HMR* in a strain containing full tDNA deletions on chromosome III even though only *HMR* has a tDNA adjacent to it, we decided to focus on the tDNA (t0) that resides immediately adjacent to *HMR* and functions as an insulator at *HMR*. Importantly, t0 lies to the right of *HMR* while the reporter gene lies to the left of *HMR*, so any effect of t0 on the transcriptional state of the reporter is not due to the barrier function of this tDNA.

To test whether t0 is necessary for regulating silencing states at *HML* and *HMR* we built a strain where only t0 was deleted on chromosome III (t0-). The lineage tree showed that this strain behaved similarly to the strain lacking all tDNAs such that both reporters were active most of the time and rarely switched to the repressed state. Like the full tDNA delete, the t0- strain showed an increased frequency of cells undergoing the transitions at both *HML* and *HMR* when compared to the wild type strain where a reporter gene that was not expressed in one generation was more likely to be expressed in the next generation.

Alternatively, to determine if the t0 tDNA was sufficient for mediating silencing effects at *HML* and *HMR*, we constructed a strain lacking 9 of the 10 tDNAs on chromosome III and where t0 is the only tDNA still present at its normal location adjacent to *HMR* (t0+). Again, we monitored expression of the reporters at *HML* and *HMR* in this background. The lineage tree showed that this strain behaved similarly to the wild type strain such that both reporters were silent more often than the full tDNA delete and t0- strains and inherited the silent state with greater fidelity.

Taken together, the data suggest that deletion of tDNAs on chromosome III had an effect on the ability of *HMR* to interact with *HML* and diminution of this clustering led to an alteration in the stability of the silenced state at these loci.

Discussion

tDNAs are middle repetitive DNA sequences scattered across all 16 chromosomes and their primary function is the synthesis of tRNAs. In this manuscript, we show that tDNAs affect local chromatin structure, which then impinges on chromosome architecture. tDNAs 1) affect chromatin structure by maintaining local nucleosome free regions along the fiber and precisely positioned nucleosomes immediately outside of the tDNAs, 2) recruit cohesins and condensins 3) affect nuclear architecture by influencing centromere clustering and 4) alter heterochromatin clustering leading to changes in the fidelity of inheritance of gene silencing.

The binding of specific proteins such as CTCF to a site on the DNA can affect nucleosome positions over long distances [96]. Nucleosome depletion at the gene and positioned nucleosomes flanking the gene is a hallmark of tDNAs [22, 24, 25, 35, 61, 97-100]. Our data show that loss of the tDNA promoters' only affect nucleosome positions in the immediate vicinity of the tDNA. The nucleosome positioning effects mediated by the tDNA bound transcription factors TFIIIC and TFIIIB are not transmitted over long distances.

tDNAs, SMC proteins and chromatin folding

The SMC proteins are involved in higher order chromosome organization in all eukaryotes and have been extensively mapped. tDNAs are binding sites for all three classes of SMC proteins (cohesin, condensin and repairsin), the SMC protein loaders Scc2 and Scc4 and the meiotic Rec8 SMC protein [28, 29, 32, 101-105]. Given these intimate connections between tDNAs and the SMC proteins our data indicate that loss of the tDNA promoters does lead to loss of SMC proteins from tDNAs but this effect is

tDNA specific since we do not see a loss of SMC proteins from centromeres or Scc2 from other sites in the genome. Surprisingly the loss of Scc2 and Brn1 from tDNAs does not affect chromatin folding. While clustering of tDNAs in the nucleus (as measured by fluorescence microscopy) is dependent upon the SMC proteins [54, 70] the precise contribution of tDNAs in this process remained unclear. Our Micro-C analysis suggests that tDNAs play a minor role in chromatin folding and tethering to nuclear substructures since we observed only subtle changes in contact frequency across the chromosome and small effects on chromosome loss rates. It is likely that tDNA independent SMC protein binding sites masks the tDNA-mediated effects. SMC proteins bind only half of the tDNAs in the nucleus and only a third of the SMC protein binding sites localize at or near tDNAs [29]. The lack of phenotype would also be consistent with previous data that showed that a reduction in the levels of the SMC proteins does not affect the properties of the chromosome arm [106]. Recently a synthetic yeast chromosome III was generated and characterized [107, 108]. The synthetic chromosome lacks repetitive sequences such as TY elements, LTRs and tRNA genes. The 3D structure of this chromosome was determined using HiC and the data show that there were no major differences between this chromosome and the wild type chromosome except for a shortening of the length. While this chromosome lacks multiple elements the three-dimensional folding data are consistent with our conclusions from the Micro-C analysis of the same chromosome lacking only tDNAs.

While it is possible that redundancy of structural elements masks tDNA-mediated effects on chromatin folding it is also possible that chromatin folding is driven by underlying DNA sequence mediated nucleosome organization and not tDNA mediated

long-range interactions. The yeast chromosomes have isochores with G-C rich, gene rich R-band segments alternating with AT-rich G-band segments [109, 110], which exhibit different functional properties and chromosome conformation [111, 112]. Chromosome III has a G-C segment from 20 to 100 kb on the left arm followed by an A-T rich central segment from 100 to 200kb on the right arm and then a second G-C rich segment from 200 to 290kb on the same arm. In this scenario, the underlying A-T rich DNA sequence likely plays a dominant role in the three dimensional folding of chromatin. tDNAs are often syntenic along chromosomes [39, 113] and it is possible that these positions have been selected for optimal gene activity rather than being involved in long-range chromatin loop formation [114]. Thus while the A-T rich isochore is structurally and functionally distinct [75, 115, 116] and is the region rich in tDNAs (See Figure1) our results would suggest that the tDNAs do not play a significant role in either tethering of this isochore or the overall folding of this segment. The tDNA clustering observed by microscopy could simply be a function of conservation of tDNA positions along the chromatin fiber.

tDNAs and centromere clustering

Chromosome tethering to nuclear substructures enables nuclear organization [1, 114] and centromeres and the telomeres along with their associated proteins play a key role in this process [7, 9, 10, 12, 15, 16, 73, 117-120]. All sixteen centromeres cluster together in a ring around the membrane-embedded spindle pole body. The centromeres are tethered to the spindle pole body via direct interactions between kinetochore-associated proteins and the spindle pole body associated microtubules in interphase [7, 73, 75, 117]. Other factors are likely to influence this phenomenon but remain unknown.

tDNA density is almost 2 fold higher in the pericentric region of *S. cerevisiae* chromosomes including chromosome III [121]. While tDNAs have been shown to help tether centromeres to the spindle axis during mitosis [121], in interphase nuclei, the loss of tDNAs results in increased interactions between the clustered centromeres. The physical presence of tDNAs in the pericentric region could interfere with the close packaging of centromeres during interphase. This could be due to transcription-mediated effects since tRNA genes are highly active. In *S. pombe,* mutations that reduce tDNA transcription result in increased tDNA association with the kinetochore and increased chromosome condensation during mitosis. Furthermore, tDNA association with kinetochores increases when these genes became inactive [55]. Thus, tDNA clustering at sites of active tRNA transcription near centromeres could hinder centromere-centromere interactions during interphase while a decrease in tDNA transcription during mitosis could help tether centromeres to the spindle axis during mitosis [121]. This would also explain the observation that the tDNA-deleted chromosome had a slightly lower chromosome loss rate.

An alternative though not mutually exclusive possibility is based on the observation that transcriptionally active tDNAs interact with nuclear pores in the G2/M phase of the cell cycle [4, 122, 123]. It is thus possible that there is a competition between pericentric tDNA- nuclear pore interactions in opposition to centromere-centromere interactions. In this scenario, the loss of tDNA tethering to the nuclear pore would enable the centromere greater freedom of movement thus enabling closer centromere-centromere interactions.

tDNA effects on *HML-HMR* interactions and the inheritance of gene silencing

633 Gene silencing is primarily a function of the Sir proteins though numerous other
634 factors influence the process [124]. Proto-silencers are sequence elements that on their
635 own are unable to silence a gene, but when located near a silencer increase the
636 efficiency of silencing [125, 126]. Our demonstration that the tDNA affects silencing of a
637 reporter adjacent to the silent *HMR* domain suggests that tDNAs function as proto-
638 silencers. Our data suggest that tDNA mediated clustering of silent loci might be
639 important in the silencing of these loci and the loss of long-range association might
640 reduce the efficient inheritance of the silent state. This is analogous to the observations
641 that gene clustering at active chromatin hubs and transcription factories increases the
642 efficiency of transcription as well as the data showing that telomere clustering increases
643 the efficiency of silencing at sub-telomeric sequences [127].
644 This unexpected observation also raises the question of how might tDNAs influence
645 long-range *HML-HMR* interactions. tDNAs, including the tDNA next to *HMR,* are sites of
646 replication slowing/pausing [86, 87, 91, 128-130]. The tDNA adjacent to *HMR* is a site
647 of replication fork pausing [89, 131]. We recently showed that long-range *HML-HMR*
648 interactions require homologous sequences to be present at these loci [19, 20] and we
649 now show that mutations in replication coupled homologous recombination repair
650 proteins including the SMC proteins, Rrm3, Top1 and Dpb3 lead to a reduction in *HML-*
651 *HMR* interactions. Based on the accumulated data we would posit that replication fork
652 slowing/pausing results in the deposition of γH2A and SMC proteins at tDNAs followed
653 by a homology search leading to *HML-HMR* interactions. The re-formation of silenced
654 chromatin following replication precludes the eviction of γH2A [132] thereby stabilizing
655 SMC protein binding, which then maintains the long-range *HML-HMR* association. The

tDNAs thus help initiate a network of interactions mediated by the SMC proteins and the Sir proteins leading to *HML-HMR* association and chromosome folding. We would like to posit that a series of transient interactions during replication aid in the setting up of the final optimal nuclear architecture found in the interphase nucleus.

In conclusion, tDNAs primarily affect local chromatin structure. Each tDNA affects nucleosome positions and protein binding in its immediate vicinity. These local perturbations functionally and structurally interact with neighboring regulatory regions resulting in tDNA mediated pleiotropic effects. In some instances tDNAs affect the expression of neighboring pol II transcribed genes by the phenomenon of local tgm silencing. In another context tDNA mediated replication pausing result in the establishment of long-range heterochromatin interactions, which then influence the inheritance of silencing states at these loci.

Acknowledgements

This work was supported in part by a grant from the NIH to RTK (GM078068) and (T32-GM008646) to JK, OH and KW. This study was funded in part by the Intramural Research Program of the National Institutes of Health (NICHD). We thank the NHLBI Core Facility for paired-end sequencing of the micrococcal nuclease libraries. The Functional Genomics Laboratory, UC Berkeley sequenced the ChIP-Seq libraries on an Illumina HiSeq4000 at the Vincent J Coates Laboratory at UC Berkeley, supported by an NIH S10 OD018174 Instrumentation Grant.

Materials and Methods

Yeast strains and primers

Table 2 and 3 list the yeast strains and the primer sequences that were used in this study.

MNase-Seq

MNase-Seq experiments were carried out as previously described [25]. In brief, isolated nuclei were digested with MNase to mono-nucleosomes. Paired-end sequencing libraries were prepared (Illumina). Paired reads (50 nt) were mapped to the reference genome (SacCer2) using Bowtie-2 [133-135]. For analysis of nucleosome occupancy (coverage) at tDNAs, both across the genome and on chromosome III, tDNAs were aligned on their start sites or at the deletion points. Data sets were normalized to their genomic average, set at 1, using only DNA fragments in the 120 to 180 bp range. In one experiment, mono-nucleosomal DNA was gel-purified, but not in the replicate, in which short fragments (< 120 bp) derived from digestion of the TFIIIB-TFIIIC complex at tDNAs (Nagarajavel 2013) were observed. The MNase-seq data are available at the GEO database:
(GSE98304 https://www.ncbi.nlm.nih.gov/geo/query/acc.cgi?token=wnynwaoqvnktfmb&acc=GSE98304)

ChIP-Seq and RNA-Seq

Chromatin immunoprecipitation reactions were performed essentially as described above but elution of the precipitated DNA from Protein A/G beads was carried out with two successive washes in 175ul of 0.1M $NaHCO_3$/1% SDS. 50ul of each input sample was diluted to 350ul with the elution buffer. NaCl was added to a final concentration of

0.2M and cross-links were reversed with an overnight incubation at 65C in a Thermomixer. All samples were treated with 60ug of RNAase A (Sigma) at 37C for 60' followed by a Proteinase K (Roche) treatment at 50C for 60'. DNA was purified with a successive phenol chloroform and chloroform extraction followed by precipitation with 2 volumes of ethanol and 50ug of glycogen (Roche).

The ChIP and Input DNA was spun, washed with 70% ethanol and re-suspended in deionized water. DNA quantitation was performed using a Qubit dsDNA HS Assay kit prior to confirmation by qPCR.

Libraries for ChIP-Seq were prepared at the Functional Genomics Laboratory, UC Berkeley and sequenced on an Illumina HiSeq4000 at the Vincent J Coates Laboratory at UC Berkeley.

For RNA-Seq, yeast strains JRY2334 and JKY690 were grown in duplicate in 50ml YPD to a cell density of 6-7x10^6 cells/ml, spun, washed in 25ml PBS, divided into 4 aliquots per culture and transferred to 1.5ml microfuge tubes. Cell pellets were flash frozen in liquid N2 and transferred to -70C. RNA, library preparation and sequencing for RNA-Seq were performed by ACGT Inc. Wheeling, IL.

Transcript abundances were estimated using Kallisto [136]. Differential analysis of gene expression data was performed using the R package Sleuth [137]. Likelihood ratio test and Wald test were used to identify the differentially expressed genes (false discovery rate adjusted p-value (or q-value) < 0.05 in both tests). Since the likelihood ratio test does not produce any metric equivalent to the fold change, we used the Wald test to generates the beta statistic, which approximates to the log2 fold change in expression between the two conditions.

Sequence data have ben deposited in the GEO database.

https://www.ncbi.nlm.nih.gov/geo/query/acc.cgi?token=krihsykczdmbpox&acc=GSE106250

ChIP

ChIP-qPCR experiments on all Brn1 and Scc2/4 were performed as previously described [20, 35]. In brief, yeast cells of a strain of interest were inoculated and grown overnight in 300 ml of YPD media to an OD of 1-2. These cells were then fixed in 1% formaldehyde for a duration of 2 hours at room temperature. The reaction was then quenched with glycine, and the cells were spun down and washed in 1X PBS. The cross linked cells were then flash frozen in dry ice and stored at -70^{0}C. In preparation for IP, the cells were thawed on ice, broken apart by bead beating, and sonicated to achieve a desired chromatin size of ~300 bp. Once the size of the chromatin was checked, cell debris was cleared from the sample by high-speed centrifugation. The cross linked, sized chromatin was split into 2 samples and IP's were done overnight in the presence of both an antibody to the protein of interest as well as pre-blocked A/G-Sepharose beads at 4^{o}C. 50 µl of input chromatin was also taken from each IP sample prior to addition of the antibody. Chromatin elution was done using 10% Chelex 100 (Bio-Rad) along with proteinase K treatment. After elution, both input and IP DNA were quantitated via a Picogreen fluorescent quantification assay (Invitrogen). For each qPCR reaction, input DNA was run in triplicate and IP DNA was run in duplicate. An equal amount of input and IP DNA was used in each individual reaction. The enrichment for a given probe was then calculated as IP/Input, and was further normalized to the OCA4 locus. The results of each ChIP-qPCR are comprised from two

746 independent crosslinks per strain assayed, and for each crosslink two independent IPs
747 were done.

748 **Mean Squared Distance Analysis**

749 Mean-squared distance analysis was carried out as previously described [68, 138, 139].
750 In brief, we built strains that contained a 64x lacO array at specific points along
751 chromosome III. We then integrated a cassette containing an spc29-RFP fusion protein
752 elsewhere in the genome. This protein is an essential kinetochore protein, and
753 therefore serves as a marker for the spindle pole body. The spindle pole body served
754 as a fixed point to which we could measure the movement of our GFP tagged loci in 3D
755 space over a period of 10 minutes. Z-stack images of the cells were taken every 30
756 seconds during the time-lapse, and the data are used to calculate the radius of
757 constraint using the equation: $<(X_t - X_{t+\Delta t})^2>$. MSD curves were generated for each
758 locus in both the WT and tDNA delete strain. The MSD curves were used to calculate
759 the radius of constraint (Rc) for each locus. This analysis was performed in no less than
760 35 cells per genotype assayed. The data were plotted in “NotBoxPlots” (source code
761 obtained from https://github.com/raacampbell/notBoxPlot)

762 ***HML-HMR* Colocalization analysis**

763 Distance assays between *HML* and *HMR* was performed as previously described [20].
764 Fluorescence microscopy was performed on live yeast cells after growing the cells in
765 YMD with Leucine, uracil, tryptophan, lysine, adenine and histidine. Cells were grown to
766 an Od A600 of approximately 0.6. Cells were washed in YMD, placed on YMD-agar
767 patches on slides, and imaged. Microscopy was performed using an Olympus xi70
768 inverted wide-field microscope with DeltaVision precision stage using a Coolsnap HQ2

camera and a 100x/1.4 oil objective. The 20 image stacks for each image were acquired with a step size of 200nm using the appropriate wavelength for CFP, YFP, GFP or mCherry. The acquisition software used was softWoRx3.7.1. The images were cropped using Adobe Photoshop. For the distance analysis between *HML* and *HMR*, the distance between the yellow and cyan dots were calculated in nanometers using the "measure" tool in three dimensions. The measured distances were loaded into R software (www.r-project.org) and the data were plotted as a box plot. The box includes the middle 50% of the data with the line in the box being the median value. The data presented are the sum of at least two independent strains.

Single Cell Expression Analysis

Single cell expression analysis was performed as previously described [93]. Briefly, cells were grown in YPD at 30C and placed in a microfluidics device. Time-lapse photos of growing cells were recorded using an Axio Observer Z1 microscope using a 40x objective. The ECYP and EYFP fluorescence intensities were normalized to the highest level of fluorescence observed and the Euchromatic mCherry signal.

Micro-C

Micro-C was performed as previously described [71]. The detailed method have been described [72]. In brief, this technique provides nucleosome level resolution of all of the interactions occurring across the genome by using MNase digestion in lieu of a restriction enzyme as in traditional Hi-C techniques. The interactome data were deposited in the GEO database GSE98543 (https://www.ncbi.nlm.nih.gov/geo/query/acc.cgi?acc=GSE98543)

Antibodies

Antibodies used in ChIP were as follows; Scc2-Myc: anti-myc 9E10 (Abcam) = 5 µl, Brn1-HA: anti-HA HA.11 (Covance) = 5 µl.

Figure Legends:

Figure 1) Drug sensitivity of wild type and tDNA delete strains

Ten-fold serial dilutions of cells starting at 10^7 cells were spotted on YPD plates with varying concentrations of various drugs and allowed to grow for between 2 and 5 days.

Figure 2) Deletion of tDNAs leads to local changes in chromatin structure

A) Comparison of nucleosome occupancy at 265 tDNAs on all of the yeast chromosomes except chromosome III. The tDNAs were aligned with respect to their transcription start sites (TSS set at 0). WT (black) tDNA delete (red).

B) Analysis of the nucleosome occupancy at tDNAs on chromosome III in the wild type and tDNA delete strain.

C) Comparison of global nucleosome phasing on chromosome III in wild type (blue line) and tDNA delete (red line) cells: average nucleosome dyad positions on 106 RNA Pol II-transcribed genes on chromosome III. These genes cover most of chromosome III. The genes were aligned with respect to their transcription start sites (TSS set at 0). The average nucleosome dyad density is set at 1.

D) MNase-seq data for wild type and tDNA delete (normalized to the genomic average (= 1)). Coverage plots are shown using all DNA fragments in the 120 to 180 bp range. The reference point (0) is the nucleotide marking the 5'-end of the deletion on chromosome III. Upstream of the deletion point at 0, the DNA sequence is the same in wild type and the tDNA delete chromosome III. Downstream of the deletion point, the DNA sequences are different. The black arrow shows the location and orientation of the

tDNA in wild type chromosome III. Meaningful plots cannot be made for two tDNAs (tP(AGG)C and tS(CGA)C), because they were moved to another chromosome. Two other tDNAs (tM(CAU)C and tK(CUU)C) are present in S288C strains but are naturally absent in W-303 strains, including the strains used here. The wild type profile is in orange and the tDNA delete profile is in blue.

Figure 3) Scc2 binding along chromosome III in the wild type and tDNA delete strain

ChIP-seq mapping of Myc-Scc2. The top panels show the distribution of Scc2 at tDNAs on chromosome III in wild type cells (left) and tDNA delete strains (right). Bottom panels show the distribution of Scc2 at 265 tDNAs on all chromosomes except chromosome III in the wild type (left) and the tDNA delete strain (right).

Figure 4) Scc2 and Brn1 binding at tDNAs on chromosome III

A) ChIP-qPCR mapping of Myc-Scc2. The data show the distribution of Scc2 at specific sites along chromosome III in the wild type and tDNA delete strain. The data are the results of two independent crosslinks from which four IP's were performed. For each amplicon, the fold enrichment compared to input was first calculated and the data were then normalized to the *OCA4* locus. An unpaired t-test assuming unequal SD was used to test for significance of differences between the wild type and tDNA delete strain.

B) ChIP-qPCR mapping of HA-Brn1, condensin. Fold enrichment and statistical significance was calculated in the same way as for the Scc2 ChIP and normalized to the *OCA4* locus.

Figure 5) Effect of tDNA deletion on chromosome III mobility

Mean square displacement analysis of seven loci along chromosome III in wild type and tDNA delete strains are shown. Box plots represent the data obtained from the MSD experiments. Components of the boxplot are as follows; red line represents the mean, pink bar is the 95% confidence interval, purple bar is the standard deviation, and the grey dots represent individual values obtained from each cell analyzed. The green arrowheads beneath the chromosome III schematic show the locations of the loci assayed. The radius of constraint (Rc) measurement was calculated from MSD graphs that were generated over the course of a 10-minute time-lapse movie. These experiments are the result of time-lapse images taken from at least 35 cells per locus assayed. A t-test was used to determine significance of differences observed between the wild type and tDNA delete strain for each loci.

Figure 6) Micro-C Interaction plots of chromosome III.

A) A snapshot of chromosome IX at 2.5kb resolution and 1kb resolution. The wild type and tDNA delete mutant is shown in the top and bottom of the contact matrix respectively.

The lower panel is a view of a segment at 100bp resolution and the insulation score are plotted above the contact matrix. The insulation score is the value obtained by calculating the number of contacts within a 10kbx10kb-sliding window using the 1kb resolution contact matrix. The local minima identify boundaries, which help demarcate CIDs.

B) A scatter plot of the insulation scores showing that there is no change in insulation strength between the wild type and tDNA delete strain.

C) The interaction decay curve for chromosome III showing that there is no significant changes between the wild type and tDNA delete strain.

D) A 4C-type contact graph using a region immediately adjacent to the deleted tRNA gene. The 1-D contact matrix at 5kb resolution was plotted. The Y-axis is the Log2 ratio of differential contacts between the wild type and tDNA delete strain.

Figure 7) Micro-C analysis of the centromeres

A) Contact map of chromosome III for the wild type and tDNA delete strain normalized by distance (obs/exp).

B) Differential contact maps were generated by dividing the tDNA matrix by the wild type matrix. Increased contacts in the tDNA delete strain are shown in red and reduced contacts in the tDNA delete strain compared to the wild type strain are shown in blue.

C) The graphs are a quantification of *CEN-CEN* interactions. The graph examines the interaction of *CEN16* with all other centromeres. The x-axis is the interaction counts of a 50 kb segment centered on each centromere (in parts per million).

D) The graph examines the interaction of *CEN3* with all other centromeres. The x-axis is the interaction counts of a 50 kb segment centered on each centromere (in parts per million). The increase in the CEN3-CEN interactions in the tDNA deletion strain was significantly higher ($p=1.22x10^{-14}$) compared to values of all CEN16-CEN interactions

879 (excluding CEN16-CEN3).

880 **Figure 8) Long-Range *HML-HMR* association**

881 A) Deletion of tDNAs on chromosome III leads to a change in *HML-HMR* interaction
882 as measured by Micro-C. Heat maps display the interaction profile between segments
883 on chromosome III that include *HML* and *HMR* (obtained from the Micro-C data).
884 Increased interactions are denoted by red and decreased interactions are denoted by
885 blue. The data are displayed in a log2 format. The x and y axes denote the region of the
886 chromosome displayed on each axis of the heat map.

887 B) Deletion of tDNA t0 leads to perturbation of *HML-HMR* long-range association.
888 The violin plots show data of the distances between *HML*::TetR-YFP and *HMR*::CFP-
889 LacI foci in asynchronously growing strains. Mann-Whitney U-Test were performed to
890 determine statistical significance between wild type and the various mutants. Wild type
891 (n=305), *sir4*Δ (n=134) ($p=6.7\ e^{-16}$), tDNA t0Δ (n=317) ($p=3.1\ e^{-14}$) or t0Δ:NL1 (n=330)
892 (p=2.2 e-^{16}) strains. The dark line in the middle represents the median distance. The
893 data for *sir4Δ* are shown as a control and are the same as those in [20].

894 C) Replication–repair proteins are necessary for *HML-HMR* interactions:
895 Violin plots of the distance between TetR-YFP and CFP-LacI foci in a given wild type
896 or mutant strain are shown. rrm3Δ (n=208) ($p=4.8\ e^{-12}$), dpb3Δ (n=134) ($p=1.7\ e^{-10}$)
897 top1Δ (n=139) ($p=4.2\ e^{-12}$) scc2D730V (n=188) ($p=1.9\ e^{-14}$). The data for the
898 *scc2D730V* allele are simply shown as a control and are the same as those in [20].

899 **Figure 9) Silencing of reporter genes at *HML* and *HMR***

A) tDNAs on chromosome III modulate silencing of reporter genes at *HML and HMR*. Representative lineage trees of the different strains that were analyzed are shown. Wild type refers to a strain containing all tDNAs on chromosome III. tDNA delete refers to a strain lacking any tDNAs on chromosome III. The expression of *HML::EYFP* or *HMR::ECFP* in each generation of cells was monitored, quantitated and is indicated by the presence of their respective colors in the cells of the tree.

B) Deletion of tDNAs on chromosome III leads to a change in the maintenance of silencing at *HML* and *HMR*. The graphs quantify the changes in expression state of *HML::EYFP* and *HMR::ECFP* between generations in the different genotypes studied. Expressed to repressed transitions identify reporters that were expressed in one generation but not expressed in the next. Repressed to expressed transitions represent reporter genes that were not expressed in one generation but expressed in the next.

Table1

Genes whose mRNA levels changed in the tDNA delete strain compared to the wild type along with statistical analysis of the differences in expression levels.

Table2

Strain list with genotypes

Table3

Sequences of PCR primers used in this study

Table4

Statistical analysis of differences in expression of HML::EYFP and HMR::ECFP in the wild type and tDNA delete strains.

References

1. Taddei, A., H. Schober, and S.M. Gasser, *The budding yeast nucleus.* Cold Spring Harb Perspect Biol, 2010. **2**(8): p. a000612.
2. Zimmer, C. and E. Fabre, *Principles of chromosomal organization: lessons from yeast.* J Cell Biol, 2011. **192**(5): p. 723-33.
3. Palladino, F., T. Laroche, E. Gilson, L. Pillus, and S.M. Gasser, *The positioning of yeast telomeres depends on SIR3, SIR4, and the integrity of the nuclear membrane.* Cold Spring Harb Symp Quant Biol, 1993. **58**: p. 733-46.
4. Ruben, G.J., J.G. Kirkland, T. Macdonough, M. Chen, R.N. Dubey, M.R. Gartenberg, and R.T. Kamakaka, *Nucleoporin Mediated Nuclear Positioning and Silencing of HMR.* PLoS One, 2011. **6**(7): p. e21923.
5. Fabre, E. and M. Spichal, *Subnuclear Architecture of telomeres and subtelomeres in yeast*, in *SubTelomeres*, E.J. Louis and M.M. Becker, Editors. 2014, Springer. p. 13-37.
6. Oakes, M., J.P. Aris, J.S. Brockenbrough, H. Wai, L. Vu, and M. Nomura, *Mutational analysis of the structure and localization of the nucleolus in the yeast Saccharomyces cerevisiae.* J Cell Biol, 1998. **143**(1): p. 23-34.
7. Jin, Q.W., J. Fuchs, and J. Loidl, *Centromere clustering is a major determinant of yeast interphase nuclear organization.* J Cell Sci, 2000. **113 (Pt 11)**: p. 1903-12.
8. Therizols, P., T. Duong, B. Dujon, C. Zimmer, and E. Fabre, *Chromosome arm length and nuclear constraints determine the dynamic relationship of yeast subtelomeres.* Proc Natl Acad Sci U S A, 2010. **107**(5): p. 2025-30.
9. Tjong, H., K. Gong, L. Chen, and F. Alber, *Physical tethering and volume exclusion determine higher-order genome organization in budding yeast.* Genome Res, 2012. **22**(7): p. 1295-305.
10. Duan, Z., M. Andronescu, K. Schutz, S. McIlwain, Y.J. Kim, C. Lee, J. Shendure, S. Fields, C.A. Blau, and W.S. Noble, *A three-dimensional model of the yeast genome.* Nature, 2010. **465**(7296): p. 363-7.
11. Palladino, F., T. Laroche, E. Gilson, A. Axelrod, L. Pillus, and S.M. Gasser, *SIR3 and SIR4 proteins are required for the positioning and integrity of yeast telomeres.* Cell, 1993. **75**: p. 543-555.
12. Andrulis, E.D., D.C. Zappulla, A. Ansari, S. Perrod, C.V. Laiosa, M.R. Gartenberg, and R. Sternglanz, *Esc1, a nuclear periphery protein required for Sir4-based plasmid anchoring and partitioning.* Mol Cell Biol, 2002. **22**(23): p. 8292-301.
13. Taddei, A., F. Hediger, F.R. Neumann, C. Bauer, and S.M. Gasser, *Separation of silencing from perinuclear anchoring functions in yeast Ku80, Sir4 and Esc1 proteins.* Embo J, 2004. **23**(6): p. 1301-12.
14. Taddei, A., M.R. Gartenberg, F.R. Neumann, F. Hediger, and S.M. Gasser, *Multiple pathways tether telomeres and silent chromatin at the nuclear periphery: functional implications for sir-mediated repression.* Novartis Found Symp, 2005. **264**: p. 140-56; discussion 156-65, 227-30.

15. Bupp, J.M., A.E. Martin, E.S. Stensrud, and S.L. Jaspersen, *Telomere anchoring at the nuclear periphery requires the budding yeast Sad1-UNC-84 domain protein Mps3.* J Cell Biol, 2007. **179**(5): p. 845-54.
16. Mekhail, K., J. Seebacher, S.P. Gygi, and D. Moazed, *Role for perinuclear chromosome tethering in maintenance of genome stability.* Nature, 2008. **456**(7222): p. 667-70.
17. Klein, F., T. Laroche, M.E. Cardenas, J.F. Hofmann, D. Schweizer, and S.M. Gasser, *Localization of RAP1 and topoisomerase II in nuclei and meiotic chromosomes of yeast.* J Cell Biol, 1992. **117**(5): p. 935-48.
18. Taddei, A., G. Van Houwe, F. Hediger, V. Kalck, F. Cubizolles, H. Schober, and S.M. Gasser, *Nuclear pore association confers optimal expression levels for an inducible yeast gene.* Nature, 2006. **441**(7094): p. 774-8.
19. Kirkland, J., M.R. Peterson, C.B. Still, L. Brueggemman, N. Dhillon, and R. Kamakaka, *Heterochromatin formation via recruitment of DNA repair proteins.* Molecular Biology of Cell, 2015.
20. Kirkland, J.G. and R.T. Kamakaka, *Long-range heterochromatin association is mediated by silencing and double-strand DNA break repair proteins.* J Cell Biol, 2013. **201**(6): p. 809-26.
21. Dieci, G., G. Fiorino, M. Castelnuovo, M. Teichmann, and A. Pagano, *The expanding RNA polymerase III transcriptome.* Trends Genet, 2007.
22. Oki, M. and R.T. Kamakaka, *Barrier Function at HMR.* Mol Cell, 2005. **19**(5): p. 707-16.
23. Weiner, A., A. Hughes, M. Yassour, O.J. Rando, and N. Friedman, *High-resolution nucleosome mapping reveals transcription-dependent promoter packaging.* Genome Res, 2010. **20**(1): p. 90-100.
24. Yuan, G.C., Y.J. Liu, M.F. Dion, M.D. Slack, L.F. Wu, S.J. Altschuler, and O.J. Rando, *Genome-scale identification of nucleosome positions in S. cerevisiae.* Science, 2005. **309**(5734): p. 626-30.
25. Cole, H.A., B.H. Howard, and D.J. Clark, *Genome-wide mapping of nucleosomes in yeast using paired-end sequencing.* Methods Enzymol, 2012. **513**: p. 145-68.
26. Geiduschek, E.P. and G.A. Kassavetis, *The RNA polymerase III transcription apparatus.* J Mol Biol, 2001. **310**(1): p. 1-26.
27. Schramm, L. and N. Hernandez, *Recruitment of RNA polymerase III to its target promoters.* Genes Dev, 2002. **16**(20): p. 2593-620.
28. Glynn, E.F., P.C. Megee, H.G. Yu, C. Mistrot, E. Unal, D.E. Koshland, J.L. DeRisi, and J.L. Gerton, *Genome-wide mapping of the cohesin complex in the yeast Saccharomyces cerevisiae.* PLoS Biol, 2004. **2**(9): p. E259.
29. D'Ambrosio, C., C.K. Schmidt, Y. Katou, G. Kelly, T. Itoh, K. Shirahige, and F. Uhlmann, *Identification of cis-acting sites for condensin loading onto budding yeast chromosomes.* Genes Dev, 2008. **22**(16): p. 2215-27.
30. Haeusler, R.A., M. Pratt-Hyatt, P.D. Good, T.A. Gipson, and D.R. Engelke, *Clustering of yeast tRNA genes is mediated by specific association of condensin with tRNA gene transcription complexes.* Genes Dev, 2008. **22**(16): p. 2204-14.
31. Lopez-Serra, L., G. Kelly, H. Patel, A. Stewart, and F. Uhlmann, *The Scc2-Scc4 complex acts in sister chromatid cohesion and transcriptional regulation by maintaining nucleosome-free regions.* Nat Genet, 2014. **46**(10): p. 1147-51.

32. Kogut, I., J. Wang, V. Guacci, R.K. Mistry, and P.C. Megee, *The Scc2/Scc4 cohesin loader determines the distribution of cohesin on budding yeast chromosomes.* Genes Dev, 2009. **23**(19): p. 2345-57.
33. Bausch, C., S. Noone, J.M. Henry, K. Gaudenz, B. Sanderson, C. Seidel, and J.L. Gerton, *Transcription alters chromosomal locations of cohesin in Saccharomyces cerevisiae.* Mol Cell Biol, 2007. **27**(24): p. 8522-32.
34. Huang, J. and B.C. Laurent, *A Role for the RSC chromatin remodeler in regulating cohesion of sister chromatid arms.* Cell Cycle, 2004. **3**(8): p. 973-5.
35. Dhillon, N., J. Raab, J. Guzzo, S.J. Szyjka, S. Gangadharan, O.M. Aparicio, B. Andrews, and R.T. Kamakaka, *DNA polymerase epsilon, acetylases and remodellers cooperate to form a specialized chromatin structure at a tRNA insulator.* Embo J, 2009. **28**(17): p. 2583-600.
36. Frenkel, F.E., M.B. Chaley, E.V. Korotkov, and K.G. Skryabin, *Evolution of tRNA-like sequences and genome variability.* Gene, 2004. **335**: p. 57-71.
37. Goodenbour, J.M. and T. Pan, *Diversity of tRNA genes in eukaryotes.* Nucleic Acids Res, 2006. **34**(21): p. 6137-46.
38. Withers, M., L. Wernisch, and M. dos Reis, *Archaeology and evolution of transfer RNA genes in the Escherichia coli genome.* Rna, 2006. **12**(6): p. 933-42.
39. Raab, J.R., J. Chiu, J. Zhu, S. Katzman, S. Kurukuti, P.A. Wade, D. Haussler, and R.T. Kamakaka, *Human tRNA genes function as chromatin insulators.* EMBO J, 2012. **31**(2): p. 330-50.
40. Wang, J., V.V. Lunyak, and I.K. Jordan, *Genome-wide prediction and analysis of human chromatin boundary elements.* Nucleic Acids Res, 2012. **40**(2): p. 511-29.
41. Van Bortle, K. and V.G. Corces, *tDNA insulators and the emerging role of TFIIIC in genome organization.* Transcription, 2012. **3**(6): p. 277-84.
42. Kirkland, J.G., J.R. Raab, and R.T. Kamakaka, *TFIIIC bound DNA elements in nuclear organization and insulation.* Biochim Biophys Acta, 2013. **1829**(3-4): p. 418-24.
43. Donze, D., C.R. Adams, J. Rine, and R.T. Kamakaka, *The boundaries of the silenced HMR domain in Saccharomyces cerevisiae.* Genes Dev, 1999. **13**(6): p. 698-708.
44. Biswas, M., N. Maqani, R. Rai, S.P. Kumaran, K.R. Iyer, E. Sendinc, J.S. Smith, and S. Laloraya, *Limiting the extent of the RDN1 heterochromatin domain by a silencing barrier and Sir2 protein levels in Saccharomyces cerevisiae.* Mol Cell Biol, 2009. **29**(10): p. 2889-98.
45. Korde, A., J.M. Rosselot, and D. Donze, *Intergenic Transcriptional Interference Is Blocked by RNA Polymerase III Transcription Factor TFIIIB in Saccharomyces cerevisiae.* Genetics, 2013. **196**(2): p. 427-38.
46. Simms, T.A., E.C. Miller, N.P. Buisson, N. Jambunathan, and D. Donze, *The Saccharomyces cerevisiae TRT2 tRNAThr gene upstream of STE6 is a barrier to repression in MATalpha cells and exerts a potential tRNA position effect in MATa cells.* Nucleic Acids Res, 2004. **32**(17): p. 5206-13.
47. Simms, T.A., S.L. Dugas, J.C. Gremillion, M.E. Ibos, M.N. Dandurand, T.T. Toliver, D.J. Edwards, and D. Donze, *TFIIIC binding sites function as both heterochromatin barriers and chromatin insulators in Saccharomyces cerevisiae.* Eukaryot Cell, 2008. **7**(12): p. 2078-86.

48. Van Bortle, K., M.H. Nichols, L. Li, C.T. Ong, N. Takenaka, Z.S. Qin, and V.G. Corces, *Insulator function and topological domain border strength scale with architectural protein occupancy.* Genome Biol, 2014. **15**(6): p. R82.
49. Ebersole, T., J.H. Kim, A. Samoshkin, N. Kouprina, A. Pavlicek, R.J. White, and V. Larionov, *tRNA genes protect a reporter gene from epigenetic silencing in mouse cells.* Cell Cycle, 2011. **10**(16): p. 2779-91.
50. Dixon, J.R., S. Selvaraj, F. Yue, A. Kim, Y. Li, Y. Shen, M. Hu, J.S. Liu, and B. Ren, *Topological domains in mammalian genomes identified by analysis of chromatin interactions.* Nature, 2012. **485**(7398): p. 376-80.
51. Good, P.D., A. Kendall, J. Ignatz-Hoover, E.L. Miller, D.A. Pai, S.R. Rivera, B. Carrick, and D.R. Engelke, *Silencing near tRNA genes is nucleosome-mediated and distinct from boundary element function.* Gene, 2013. **526**(1): p. 7-15.
52. Thompson, M., R.A. Haeusler, P.D. Good, and D.R. Engelke, *Nucleolar clustering of dispersed tRNA genes.* Science, 2003. **302**(5649): p. 1399-401.
53. Pombo, A., D.A. Jackson, M. Hollinshead, Z. Wang, R.G. Roeder, and P.R. Cook, *Regional specialization in human nuclei: visualization of discrete sites of transcription by RNA polymerase III.* Embo J, 1999. **18**(8): p. 2241-53.
54. Haeusler, R.A. and D.R. Engelke, *Spatial organization of transcription by RNA polymerase III.* Nucleic Acids Res, 2006. **34**(17): p. 4826-36.
55. Iwasaki, O., A. Tanaka, H. Tanizawa, S.I. Grewal, and K. Noma, *Centromeric localization of dispersed Pol III genes in fission yeast.* Mol Biol Cell, 2010. **21**(2): p. 254-65.
56. Schalbetter, S.A., A. Goloborodko, G. Fudenberg, J.M. Belton, C. Miles, M. Yu, J. Dekker, L. Mirny, and J. Baxter, *SMC complexes differentially compact mitotic chromosomes according to genomic context.* Nat Cell Biol, 2017. **19**(9): p. 1071-1080.
57. Haeusler, R.A. and D.R. Engelke, *Genome organization in three dimensions: thinking outside the line.* Cell Cycle, 2004. **3**(3): p. 273-5.
58. Iwasaki, O. and K. Noma, *Global genome organization mediated by RNA polymerase III-transcribed genes in fission yeast.* Gene, 2012. **493**(2): p. 195-200.
59. Ho, C.K. and J. Abelson, *Testing for intron function in the essential Saccharomyces cerevisiae tRNA(SerUCG) gene.* J Mol Biol, 1988. **202**(3): p. 667-72.
60. Bloom-Ackermann, Z., S. Navon, H. Gingold, R. Towers, Y. Pilpel, and O. Dahan, *A comprehensive tRNA deletion library unravels the genetic architecture of the tRNA pool.* PLoS Genet, 2014. **10**(1): p. e1004084.
61. Dion, M.F., T. Kaplan, M. Kim, S. Buratowski, N. Friedman, and O.J. Rando, *Dynamics of replication-independent histone turnover in budding yeast.* Science, 2007. **315**(5817): p. 1405-8.
62. Chereji, R.V., J. Ocampo, and D.J. Clark, *MNase-Sensitive Complexes in Yeast: Nucleosomes and Non-histone Barriers.* Mol Cell, 2017. **65**(3): p. 565-577 e3.
63. Uhlmann, F., *SMC complexes: from DNA to chromosomes.* Nat Rev Mol Cell Biol, 2016. **17**(7): p. 399-412.
64. Parnell, T.J., J.T. Huff, and B.R. Cairns, *RSC regulates nucleosome positioning at Pol II genes and density at Pol III genes.* Embo J, 2008. **27**(1): p. 100-10.

65. Damelin, M., I. Simon, T.I. Moy, B. Wilson, S. Komili, P. Tempst, F.P. Roth, R.A. Young, B.R. Cairns, and P.A. Silver, *The genome-wide localization of Rsc9, a component of the RSC chromatin-remodeling complex, changes in response to stress.* Mol Cell, 2002. **9**(3): p. 563-73.
66. Dion, V., V. Kalck, C. Horigome, B.D. Towbin, and S.M. Gasser, *Increased mobility of double-strand breaks requires Mec1, Rad9 and the homologous recombination machinery.* Nat Cell Biol, 2012.
67. Mine-Hattab, J. and R. Rothstein, *Increased chromosome mobility facilitates homology search during recombination.* Nat Cell Biol, 2012.
68. Verdaasdonk, J.S., P.A. Vasquez, R.M. Barry, T. Barry, S. Goodwin, M.G. Forest, and K. Bloom, *Centromere tethering confines chromosome domains.* Mol Cell, 2013. **52**(6): p. 819-31.
69. Albert, B., J. Mathon, A. Shukla, H. Saad, C. Normand, I. Leger-Silvestre, D. Villa, A. Kamgoue, J. Mozziconacci, H. Wong, C. Zimmer, P. Bhargava, A. Bancaud, and O. Gadal, *Systematic characterization of the conformation and dynamics of budding yeast chromosome XII.* J Cell Biol, 2013. **202**(2): p. 201-10.
70. Noma, K., H.P. Cam, R.J. Maraia, and S.I. Grewal, *A role for TFIIIC transcription factor complex in genome organization.* Cell, 2006. **125**(5): p. 859-72.
71. Hsieh, T.H., A. Weiner, B. Lajoie, J. Dekker, N. Friedman, and O.J. Rando, *Mapping Nucleosome Resolution Chromosome Folding in Yeast by Micro-C.* Cell, 2015. **162**(1): p. 108-19.
72. Hsieh, T.S., G. Fudenberg, A. Goloborodko, and O.J. Rando, *Micro-C XL: assaying chromosome conformation from the nucleosome to the entire genome.* Nat Methods, 2016. **13**(12): p. 1009-1011.
73. Guacci, V., E. Hogan, and D. Koshland, *Centromere position in budding yeast: evidence for anaphase A.* Mol Biol Cell, 1997. **8**(6): p. 957-72.
74. Jin, Q., E. Trelles-Sticken, H. Scherthan, and J. Loidl, *Yeast nuclei display prominent centromere clustering that is reduced in nondividing cells and in meiotic prophase.* J Cell Biol, 1998. **141**(1): p. 21-9.
75. Dekker, J., K. Rippe, M. Dekker, and N. Kleckner, *Capturing chromosome conformation.* Science, 2002. **295**(5558): p. 1306-11.
76. Kumaran, R., S.Y. Yang, and J.Y. Leu, *Characterization of chromosome stability in diploid, polyploid and hybrid yeast cells.* PLoS One, 2013. **8**(7): p. e68094.
77. Miele, A., K. Bystricky, and J. Dekker, *Yeast silent mating type loci form heterochromatic clusters through silencer protein-dependent long-range interactions.* PLoS Genet, 2009. **5**(5): p. e1000478.
78. Dubarry, M., I. Loiodice, C.L. Chen, C. Thermes, and A. Taddei, *Tight protein-DNA interactions favor gene silencing.* Genes Dev, 2011. **25**(13): p. 1365-70.
79. Giorgetti, L. and E. Heard, *Closing the loop: 3C versus DNA FISH.* Genome Biol, 2016. **17**(1): p. 215.
80. Fraser, J., I. Williamson, W.A. Bickmore, and J. Dostie, *An Overview of Genome Organization and How We Got There: from FISH to Hi-C.* Microbiol Mol Biol Rev, 2015. **79**(3): p. 347-72.
81. Williamson, I., S. Berlivet, R. Eskeland, S. Boyle, R.S. Illingworth, D. Paquette, J. Dostie, and W.A. Bickmore, *Spatial genome organization: contrasting views from*

chromosome conformation capture and fluorescence in situ hybridization. Genes Dev, 2014. **28**(24): p. 2778-91.
82. Dubey, R.N. and M.R. Gartenberg, *A tDNA establishes cohesion of a neighboring silent chromatin domain.* Genes Dev, 2007. **21**(17): p. 2150-60.
83. Donze, D. and R.T. Kamakaka, *RNA polymerase III and RNA polymerase II promoter complexes are heterochromatin barriers in Saccharomyces cerevisiae.* Embo J, 2001. **20**(3): p. 520-31.
84. Valenzuela, L., N. Dhillon, and R.T. Kamakaka, *Transcription independent insulation at TFIIIC-dependent insulators.* Genetics, 2009. **183**(1): p. 131-48.
85. Dilworth, D.J., A.J. Tackett, R.S. Rogers, E.C. Yi, R.H. Christmas, J.J. Smith, A.F. Siegel, B.T. Chait, R.W. Wozniak, and J.D. Aitchison, *The mobile nucleoporin Nup2p and chromatin-bound Prp20p function in endogenous NPC-mediated transcriptional control.* J Cell Biol, 2005. **171**(6): p. 955-65.
86. Deshpande, A.M. and C.S. Newlon, *DNA replication fork pause sites dependent on transcription.* Science, 1996. **272**(5264): p. 1030-3.
87. Azvolinsky, A., P.G. Giresi, J.D. Lieb, and V.A. Zakian, *Highly transcribed RNA polymerase II genes are impediments to replication fork progression in Saccharomyces cerevisiae.* Mol Cell, 2009. **34**(6): p. 722-34.
88. Achar, Y.J. and M. Foiani, *Coordinating Replication with Transcription.* Adv Exp Med Biol, 2017. **1042**: p. 455-487.
89. Szilard, R.K., P.E. Jacques, L. Laramee, B. Cheng, S. Galicia, A.R. Bataille, M. Yeung, M. Mendez, M. Bergeron, F. Robert, and D. Durocher, *Systematic identification of fragile sites via genome-wide location analysis of gamma-H2AX.* Nat Struct Mol Biol, 2010. **17**(3): p. 299-305.
90. Lengronne, A., Y. Katou, S. Mori, S. Yokobayashi, G.P. Kelly, T. Itoh, Y. Watanabe, K. Shirahige, and F. Uhlmann, *Cohesin relocation from sites of chromosomal loading to places of convergent transcription.* Nature, 2004. **430**(6999): p. 573-8.
91. Ivessa, A.S., B.A. Lenzmeier, J.B. Bessler, L.K. Goudsouzian, S.L. Schnakenberg, and V.A. Zakian, *The Saccharomyces cerevisiae helicase Rrm3p facilitates replication past nonhistone protein-DNA complexes.* Mol Cell, 2003. **12**(6): p. 1525-36.
92. Azvolinsky, A., S. Dunaway, J.Z. Torres, J.B. Bessler, and V.A. Zakian, *The S. cerevisiae Rrm3p DNA helicase moves with the replication fork and affects replication of all yeast chromosomes.* Genes Dev, 2006. **20**(22): p. 3104-16.
93. Mano, Y., T.J. Kobayashi, J. Nakayama, H. Uchida, and M. Oki, *Single cell visualization of yeast gene expression shows correlation of epigenetic switching between multiple heterochromatic regions through multiple generations.* PLoS Biol, 2013. **11**(7): p. e1001601.
94. Valenzuela, L., S. Gangadharan, and R.T. Kamakaka, *Analyses of SUM1-1-mediated long-range repression.* Genetics, 2006. **172**(1): p. 99-112.
95. Valenzuela, L., N. Dhillon, R.N. Dubey, M.R. Gartenberg, and R.T. Kamakaka, *Long-range communication between the silencers of HMR.* Mol Cell Biol, 2008. **28**(6): p. 1924-35.

96. Fu, Y., M. Sinha, C.L. Peterson, and Z. Weng, *The insulator binding protein CTCF positions 20 nucleosomes around its binding sites across the human genome.* PLoS Genet, 2008. **4**(7): p. e1000138.
97. Nagarajavel, V., J.R. Iben, B.H. Howard, R.J. Maraia, and D.J. Clark, *Global 'bootprinting' reveals the elastic architecture of the yeast TFIIIB-TFIIIC transcription complex in vivo.* Nucleic Acids Res, 2013. **41**(17): p. 8135-43.
98. Roberts, D.N., A.J. Stewart, J.T. Huff, and B.R. Cairns, *The RNA polymerase III transcriptome revealed by genome-wide localization and activity-occupancy relationships.* Proc Natl Acad Sci U S A, 2003. **100**(25): p. 14695-700.
99. Moqtaderi, Z. and K. Struhl, *Genome-wide occupancy profile of the RNA polymerase III machinery in Saccharomyces cerevisiae reveals loci with incomplete transcription complexes.* Mol Cell Biol, 2004. **24**(10): p. 4118-27.
100. Harismendy, O., C.G. Gendrel, P. Soularue, X. Gidrol, A. Sentenac, M. Werner, and O. Lefebvre, *Genome-wide location of yeast RNA polymerase III transcription machinery.* Embo J, 2003. **22**(18): p. 4738-47.
101. Blat, Y. and N. Kleckner, *Cohesins bind to preferential sites along yeast chromosome III, with differential regulation along arms versus the centric region.* Cell, 1999. **98**(2): p. 249-59.
102. Laloraya, S., V. Guacci, and D. Koshland, *Chromosomal addresses of the cohesin component Mcd1p.* J Cell Biol, 2000. **151**(5): p. 1047-56.
103. Lindroos, H.B., L. Strom, T. Itoh, Y. Katou, K. Shirahige, and C. Sjogren, *Chromosomal association of the Smc5/6 complex reveals that it functions in differently regulated pathways.* Mol Cell, 2006. **22**(6): p. 755-67.
104. Klein, F., P. Mahr, M. Galova, S.B. Buonomo, C. Michaelis, K. Nairz, and K. Nasmyth, *A central role for cohesins in sister chromatid cohesion, formation of axial elements, and recombination during yeast meiosis.* Cell, 1999. **98**(1): p. 91-103.
105. Noma, K.I., *The Yeast Genomes in Three Dimensions: Mechanisms and Functions.* Annu Rev Genet, 2017.
106. Heidinger-Pauli, J.M., O. Mert, C. Davenport, V. Guacci, and D. Koshland, *Systematic reduction of cohesin differentially affects chromosome segregation, condensation, and DNA repair.* Curr Biol, 2010. **20**(10): p. 957-63.
107. Annaluru, N., H. Muller, L.A. Mitchell, S. Ramalingam, G. Stracquadanio, S.M. Richardson, J.S. Dymond, Z. Kuang, L.Z. Scheifele, E.M. Cooper, Y. Cai, K. Zeller, N. Agmon, J.S. Han, M. Hadjithomas, J. Tullman, K. Caravelli, K. Cirelli, Z. Guo, V. London, A. Yeluru, S. Murugan, K. Kandavelou, N. Agier, G. Fischer, K. Yang, J.A. Martin, M. Bilgel, P. Bohutski, K.M. Boulier, B.J. Capaldo, J. Chang, K. Charoen, W.J. Choi, P. Deng, J.E. DiCarlo, J. Doong, J. Dunn, J.I. Feinberg, C. Fernandez, C.E. Floria, D. Gladowski, P. Hadidi, I. Ishizuka, J. Jabbari, C.Y. Lau, P.A. Lee, S. Li, D. Lin, M.E. Linder, J. Ling, J. Liu, J. Liu, M. London, H. Ma, J. Mao, J.E. McDade, A. McMillan, A.M. Moore, W.C. Oh, Y. Ouyang, R. Patel, M. Paul, L.C. Paulsen, J. Qiu, A. Rhee, M.G. Rubashkin, I.Y. Soh, N.E. Sotuyo, V. Srinivas, A. Suarez, A. Wong, R. Wong, W.R. Xie, Y. Xu, A.T. Yu, R. Koszul, J.S. Bader, J.D. Boeke, and S. Chandrasegaran, *Total synthesis of a functional designer eukaryotic chromosome.* Science, 2014. **344**(6179): p. 55-8.

108. Mercy, G., J. Mozziconacci, V.F. Scolari, K. Yang, G. Zhao, A. Thierry, Y. Luo, L.A. Mitchell, M. Shen, Y. Shen, R. Walker, W. Zhang, Y. Wu, Z.X. Xie, Z. Luo, Y. Cai, J. Dai, H. Yang, Y.J. Yuan, J.D. Boeke, J.S. Bader, H. Muller, and R. Koszul, *3D organization of synthetic and scrambled chromosomes.* Science, 2017. **355**(6329).
109. Dujon, B., *The yeast genome project: what did we learn?* Trends in Genet., 1996. **12**(7): p. 263-270.
110. Sharp, P.M. and A.T. Lloyd, *Regional base composition variation along yeast chromosome III: evolution of chromosome primary structure.* Nucleic Acids Res, 1993. **21**(2): p. 179-83.
111. Dekker, J., *GC- and AT-rich chromatin domains differ in conformation and histone modification status and are differentially modulated by Rpd3p.* Genome Biol, 2007. **8**(6): p. R116.
112. Blat, Y., R.U. Protacio, N. Hunter, and N. Kleckner, *Physical and functional interactions among basic chromosome organizational features govern early steps of meiotic chiasma formation.* Cell, 2002. **111**(6): p. 791-802.
113. Raab, J.R. and R.T. Kamakaka, *Insulators and promoters: closer than we think.* Nat Rev Genet, 2010. **11**(6): p. 439-46.
114. Gehlen, L.R., G. Gruenert, M.B. Jones, C.D. Rodley, J. Langowski, and J.M. O'Sullivan, *Chromosome positioning and the clustering of functionally related loci in yeast is driven by chromosomal interactions.* Nucleus, 2012. **3**(4): p. 370-83.
115. Baudat, F. and A. Nicolas, *Clustering of meiotic double-strand breaks on yeast chromosome III.* Proc Natl Acad Sci U S A, 1997. **94**(10): p. 5213-8.
116. Gerton, J.L., J. DeRisi, R. Shroff, M. Lichten, P.O. Brown, and T.D. Petes, *Global mapping of meiotic recombination hotspots and coldspots in the yeast Saccharomyces cerevisiae.* Proc Natl Acad Sci U S A, 2000. **97**(21): p. 11383-90.
117. Bystricky, K., P. Heun, L. Gehlen, J. Langowski, and S.M. Gasser, *Long-range compaction and flexibility of interphase chromatin in budding yeast analyzed by high-resolution imaging techniques.* Proc Natl Acad Sci U S A, 2004. **101**(47): p. 16495-500.
118. Gartenberg, M.R., F.R. Neumann, T. Laroche, M. Blaszczyk, and S.M. Gasser, *Sir-mediated repression can occur independently of chromosomal and subnuclear contexts.* Cell, 2004. **119**(7): p. 955-67.
119. Taddei, A. and S.M. Gasser, *Multiple pathways for telomere tethering: functional implications of subnuclear position for heterochromatin formation.* Biochim Biophys Acta, 2004. **1677**(1-3): p. 120-8.
120. Schober, H., H. Ferreira, V. Kalck, L.R. Gehlen, and S.M. Gasser, *Yeast telomerase and the SUN domain protein Mps3 anchor telomeres and repress subtelomeric recombination.* Genes Dev, 2009. **23**(8): p. 928-38.
121. Snider, C.E., A.D. Stephens, J.G. Kirkland, O. Hamdani, R.T. Kamakaka, and K. Bloom, *Dyskerin, tRNA genes, and condensin tether pericentric chromatin to the spindle axis in mitosis.* J Cell Biol, 2014. **207**(2): p. 189-99.
122. Casolari, J.M., C.R. Brown, S. Komili, J. West, H. Hieronymus, and P.A. Silver, *Genome-wide localization of the nuclear transport machinery couples transcriptional status and nuclear organization.* Cell, 2004. **117**(4): p. 427-39.

123. Chen, M. and M.R. Gartenberg, *Coordination of tRNA transcription with export at nuclear pore complexes in budding yeast.* Genes Dev, 2014. **28**(9): p. 959-70.
124. Gartenberg, M.R. and J.S. Smith, *The Nuts and Bolts of Transcriptionally Silent Chromatin in Saccharomyces cerevisiae.* Genetics, 2016. **203**(4): p. 1563-99.
125. Fourel, G., E. Lebrun, and E. Gilson, *Protosilencers as building blocks for heterochromatin.* Bioessays, 2002. **24**(9): p. 828-35.
126. Lebrun, E., E. Revardel, C. Boscheron, R. Li, E. Gilson, and G. Fourel, *Protosilencers in Saccharomyces cerevisiae subtelomeric regions.* Genetics, 2001. **158**(1): p. 167-76.
127. Gasser, S.M., F. Hediger, A. Taddei, F.R. Neumann, and M.R. Gartenberg, *The function of telomere clustering in yeast: the circe effect.* Cold Spring Harb Symp Quant Biol, 2004. **69**: p. 327-37.
128. Wang, Y., M. Vujcic, and D. Kowalski, *DNA replication forks pause at silent origins near the HML locus in budding yeast.* Mol Cell Biol, 2001. **21**(15): p. 4938-48.
129. Lemoine, F.J., N.P. Degtyareva, K. Lobachev, and T.D. Petes, *Chromosomal translocations in yeast induced by low levels of DNA polymerase a model for chromosome fragile sites.* Cell, 2005. **120**(5): p. 587-98.
130. Admire, A., L. Shanks, N. Danzl, M. Wang, U. Weier, W. Stevens, E. Hunt, and T. Weinert, *Cycles of chromosome instability are associated with a fragile site and are increased by defects in DNA replication and checkpoint controls in yeast.* Genes Dev, 2006. **20**(2): p. 159-73.
131. Kitada, T., T. Schleker, A.S. Sperling, W. Xie, S.M. Gasser, and M. Grunstein, *gammaH2A is a component of yeast heterochromatin required for telomere elongation.* Cell Cycle, 2011. **10**(2): p. 293-300.
132. Keogh, M.C., J.A. Kim, M. Downey, J. Fillingham, D. Chowdhury, J.C. Harrison, M. Onishi, N. Datta, S. Galicia, A. Emili, J. Lieberman, X. Shen, S. Buratowski, J.E. Haber, D. Durocher, J.F. Greenblatt, and N.J. Krogan, *A phosphatase complex that dephosphorylates gammaH2AX regulates DNA damage checkpoint recovery.* Nature, 2006. **439**(7075): p. 497-501.
133. Cole, H.A., J. Ocampo, J.R. Iben, R.V. Chereji, and D.J. Clark, *Heavy transcription of yeast genes correlates with differential loss of histone H2B relative to H4 and queued RNA polymerases.* Nucleic Acids Res, 2014. **42**(20): p. 12512-22.
134. Ocampo, J., R.V. Chereji, P.R. Eriksson, and D.J. Clark, *The ISW1 and CHD1 ATP-dependent chromatin remodelers compete to set nucleosome spacing in vivo.* Nucleic Acids Res, 2016. **44**(10): p. 4625-35.
135. Langmead, B. and S.L. Salzberg, *Fast gapped-read alignment with Bowtie 2.* Nat Methods, 2012. **9**(4): p. 357-9.
136. Bray, N.L., H. Pimentel, P. Melsted, and L. Pachter, *Near-optimal probabilistic RNA-seq quantification.* Nat Biotechnol, 2016. **34**(5): p. 525-7.
137. Pimentel, H., N.L. Bray, S. Puente, P. Melsted, and L. Pachter, *Differential analysis of RNA-seq incorporating quantification uncertainty.* Nat Methods, 2017. **14**(7): p. 687-690.

138. Hediger, F., F.R. Neumann, G. Van Houwe, K. Dubrana, and S.M. Gasser, *Live Imaging of Telomeres. yKu and Sir Proteins Define Redundant Telomere-Anchoring Pathways in Yeast.* Curr Biol, 2002. **12**(24): p. 2076-89.
139. Heun, P., T. Laroche, K. Shimada, P. Furrer, and S.M. Gasser, *Chromosome dynamics in the yeast interphase nucleus.* Science, 2001. **294**(5549): p. 2181-6.

Figure 1

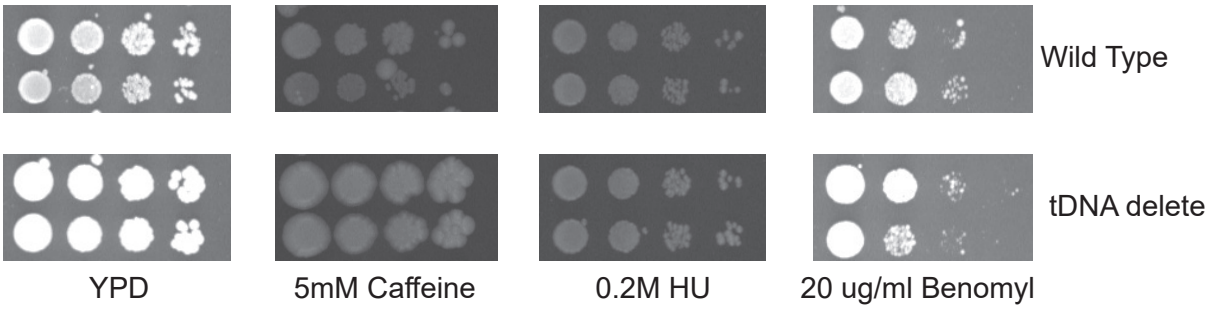
Wild Type
tDNA delete
YPD
5mM Caffeine
0.2M HU
20 ug/ml Benomyl

Figure 2

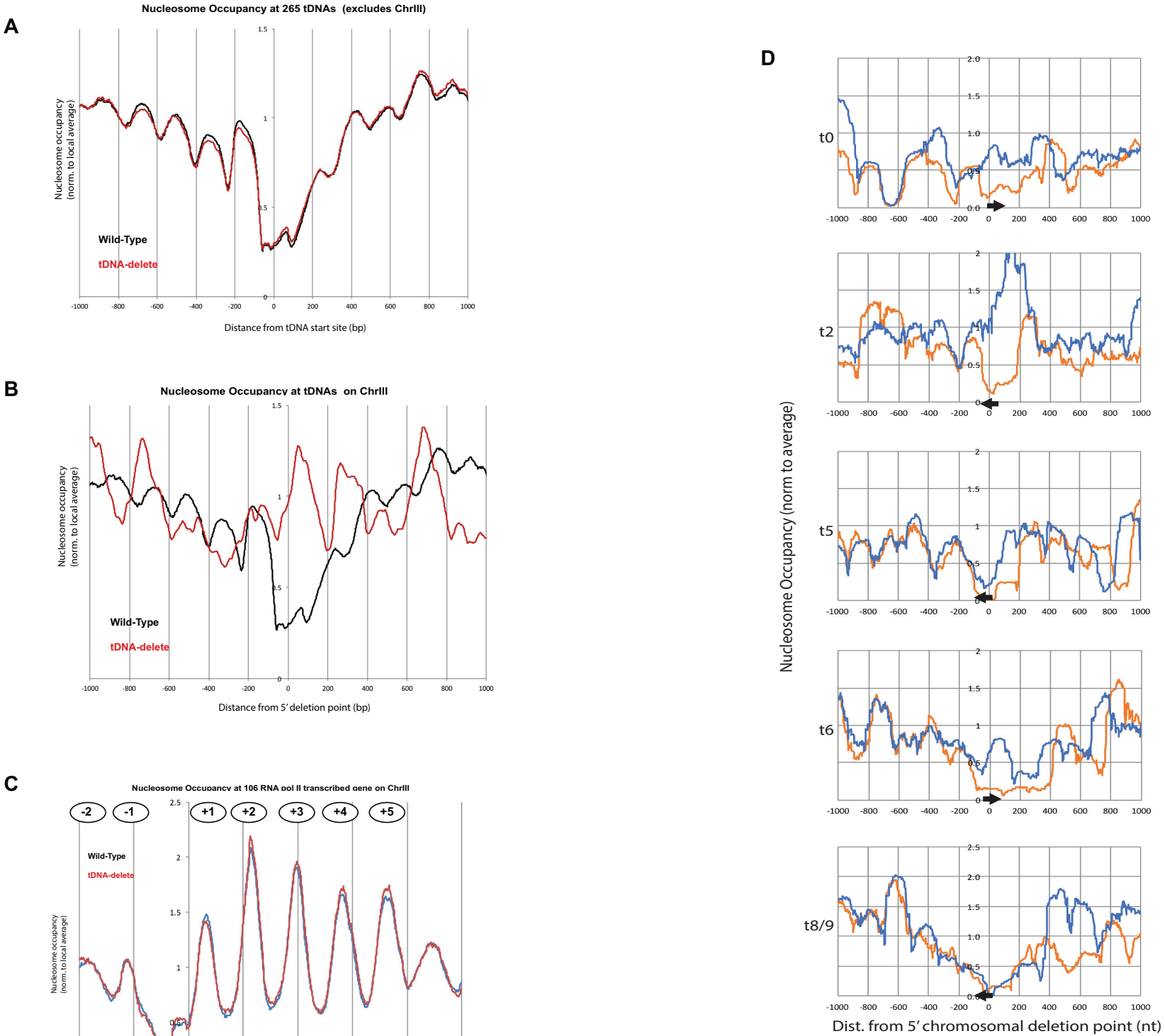
A
Nucleosome Occupancy at 265 tDNAs (excludes ChrIII)
Nucleosome occupancy (norm. to local average)
Wild-Type
tDNA-delete
Distance from tDNA start site (bp)
B
Nucleosome Occupancy at tDNAs on ChrIII
Nucleosome occupancy (norm. to local average)
Wild-Type
tDNA-delete
Distance from 5′ deletion point (bp)
C
Nucleosome Occupancy at 106 RNA pol II transcribed gene on ChrIII
-2
-1
+1
+2
+3
+4
+5
Wild-Type
tDNA-delete
Nucleosome occupancy (norm. to local average)
Distance from TSS (bp)
D
t0
t2
t5
t6
t8/9
Nucleosome Occupancy (norm to average)
Dist. from 5′ chromosomal deletion point (nt)

Figure 3

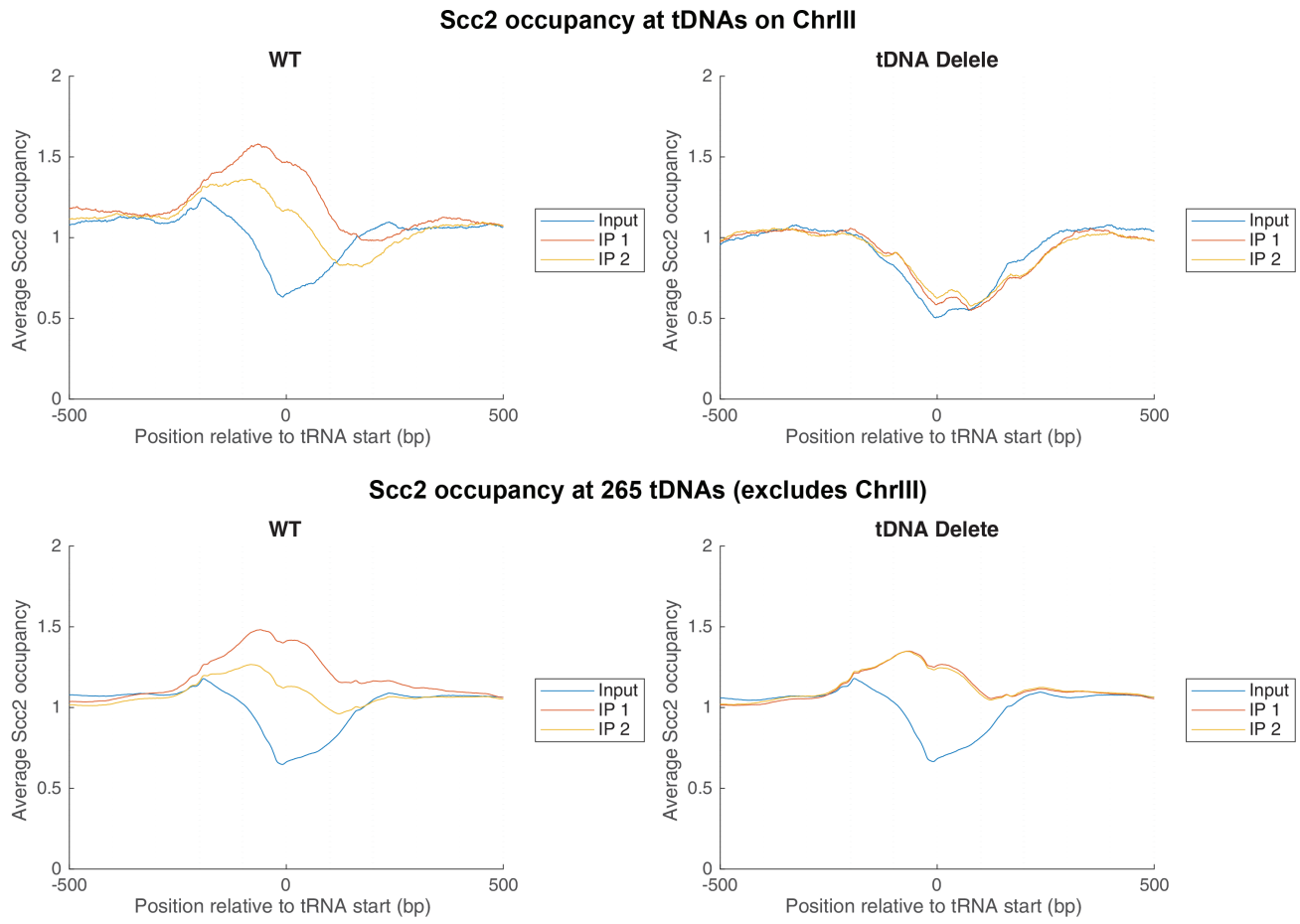
Scc2 occupancy at tDNAs on ChrIII
WT
tDNA Delele
Average Scc2 occupancy
Position relative to tRNA start (bp)
Input
IP 1
IP 2
Scc2 occupancy at 265 tDNAs (excludes ChrIII)
WT
tDNA Delete
Average Scc2 occupancy
Position relative to tRNA start (bp)
Input
IP 1
IP 2

Figure 4A

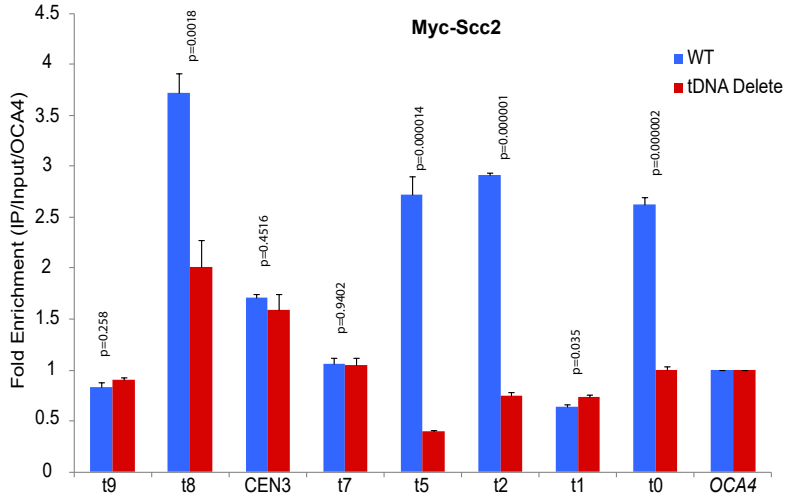

Figure 4B

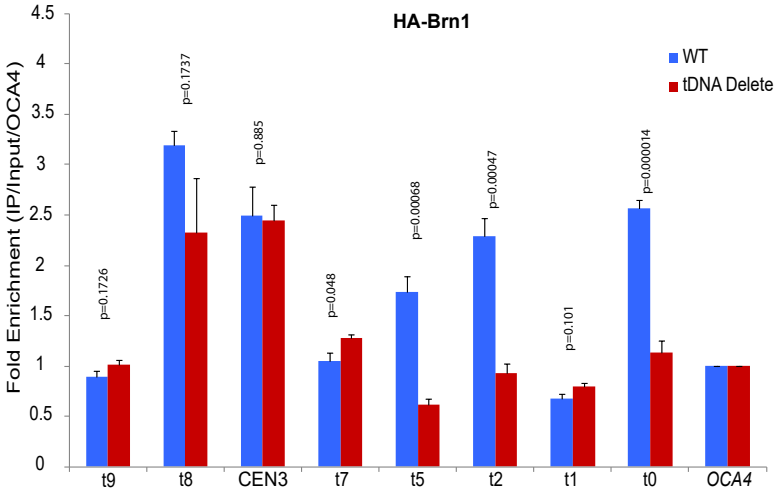

Figure 5

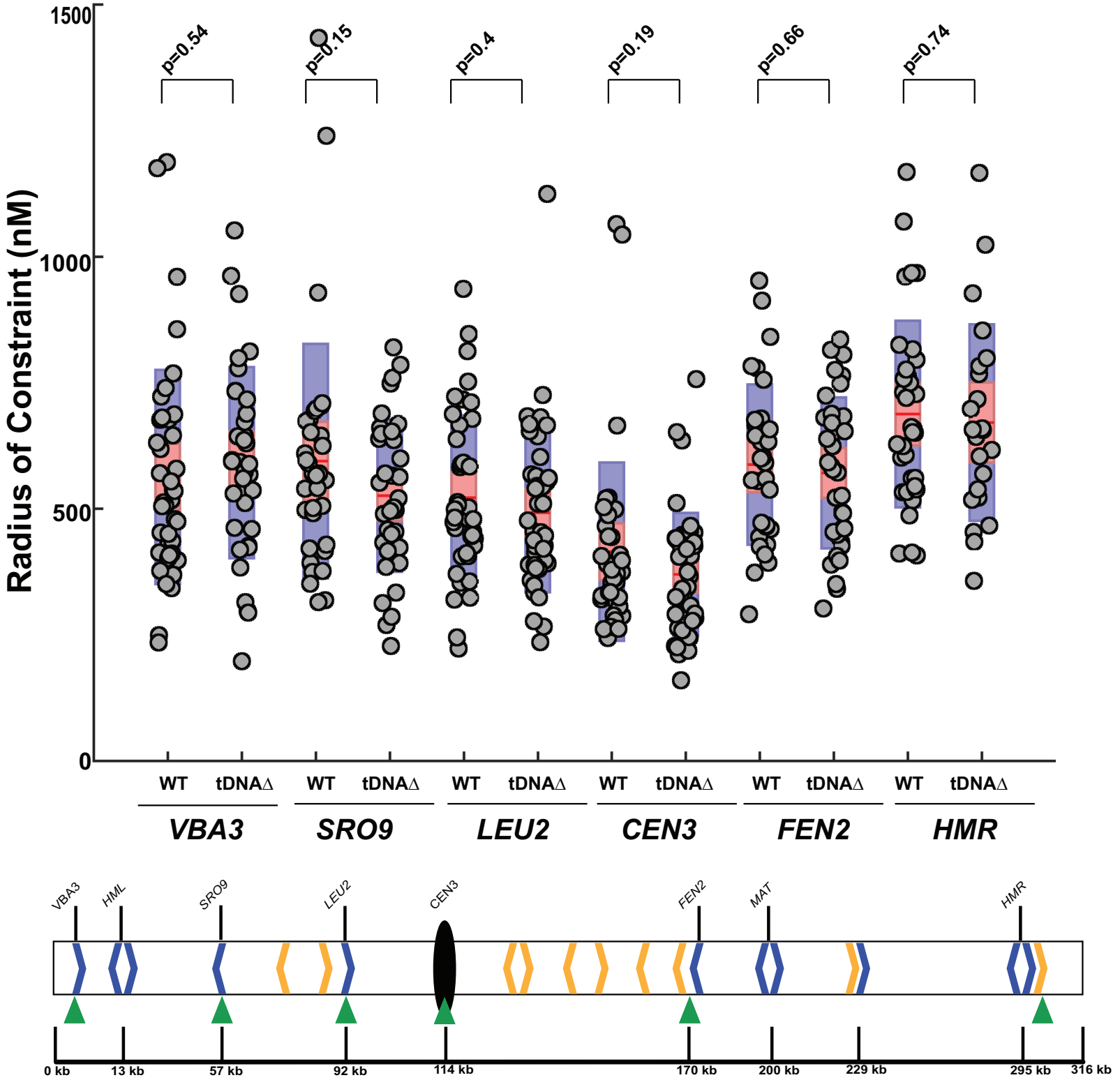
Radius of Constraint (nM)
1500
1000
500
0
p=0.54
p=0.15
p=0.4
p=0.19
p=0.66
p=0.74
WT
tDNAΔ
VBA3
SRO9
LEU2
CEN3
FEN2
HMR
VBA3
HML
SRO9
LEU2
CEN3
FEN2
MAT
HMR
0 kb
13 kb
57 kb
92 kb
114 kb
170 kb
200 kb
229 kb
295 kb
316 kb

Figure 6

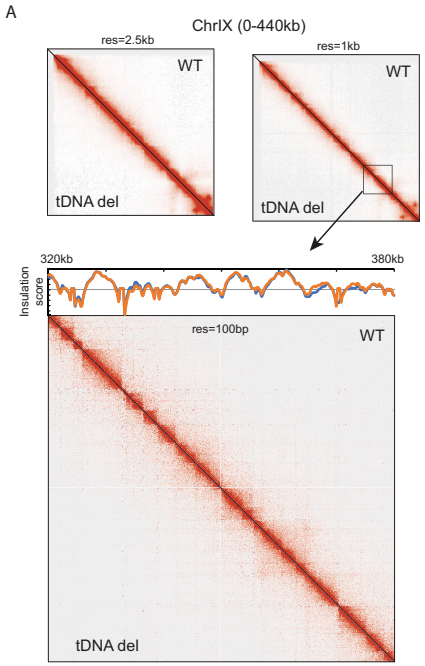
A
ChrIX (0-440kb)
res=2.5kb
WT
tDNA del
res=1kb
WT
tDNA del
320kb
380kb
Insulation score
res=100bp
WT
tDNA del

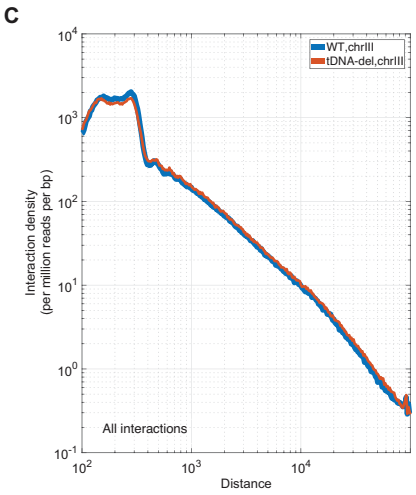
C
WT,chrIII
tDNA-del,chrIII
Interaction density (per million reads per bp)
All interactions
Distance

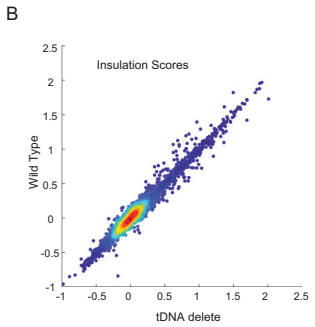
B
Insulation Scores
Wild Type
tDNA delete

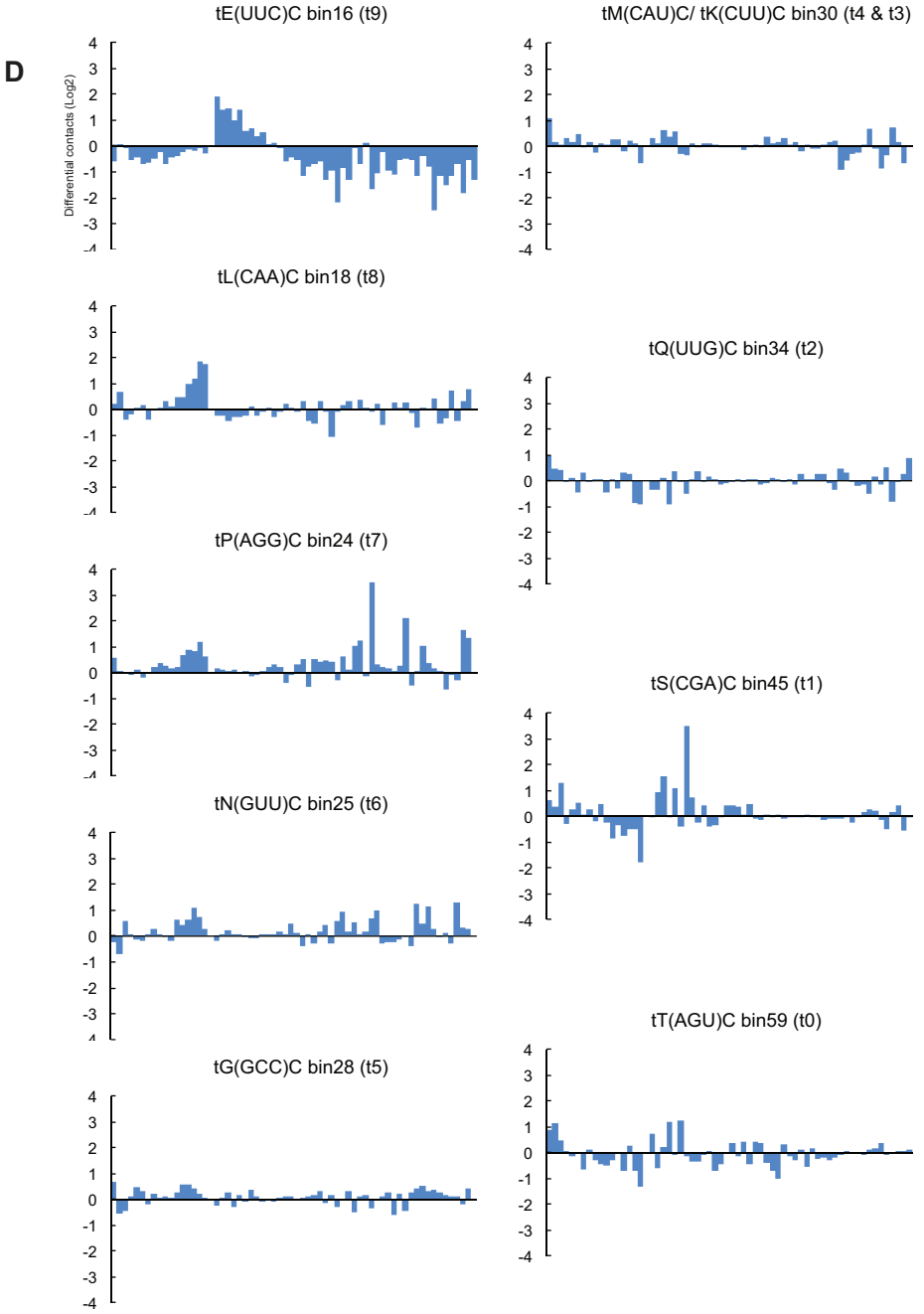
D
tE(UUC)C bin16 (t9)
tM(CAU)C/ tK(CUU)C bin30 (t4 & t3)
Differential contacts (Log2)
tL(CAA)C bin18 (t8)
tQ(UUG)C bin34 (t2)
tP(AGG)C bin24 (t7)
tS(CGA)C bin45 (t1)
tN(GUU)C bin25 (t6)
tT(AGU)C bin59 (t0)
tG(GCC)C bin28 (t5)

Figure 7

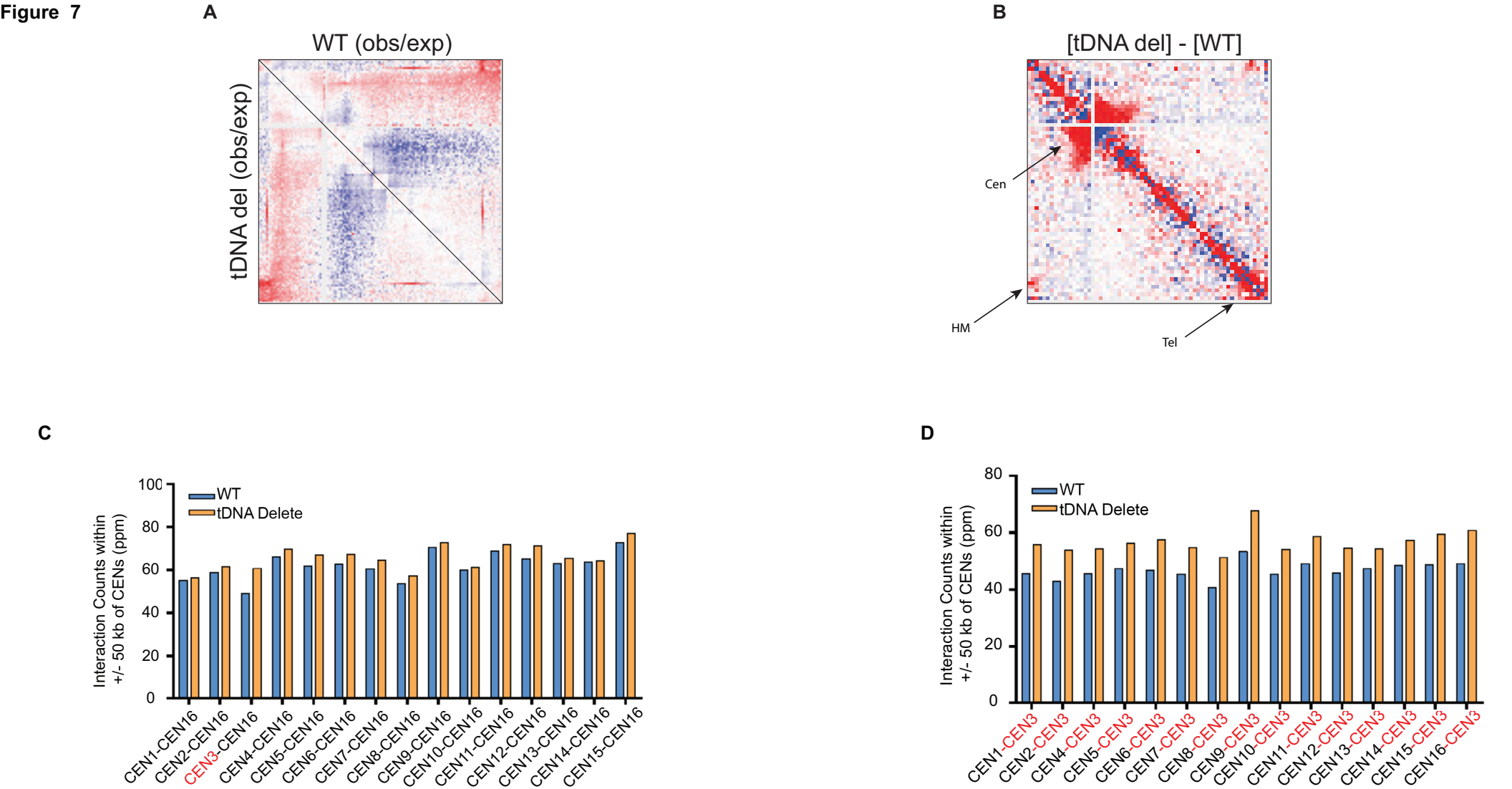
A
WT (obs/exp)
tDNA del (obs/exp)
B
[tDNA del] - [WT]
Cen
HM
Tel
C
Interaction Counts within +/- 50 kb of CENs (ppm)
WT
tDNA Delete
CEN1-CEN16
CEN2-CEN16
CEN3-CEN16
CEN4-CEN16
CEN5-CEN16
CEN6-CEN16
CEN7-CEN16
CEN8-CEN16
CEN9-CEN16
CEN10-CEN16
CEN11-CEN16
CEN12-CEN16
CEN13-CEN16
CEN14-CEN16
CEN15-CEN16
D
Interaction Counts within +/- 50 kb of CENs (ppm)
WT
tDNA Delete
CEN1-CEN3
CEN2-CEN3
CEN4-CEN3
CEN5-CEN3
CEN6-CEN3
CEN7-CEN3
CEN8-CEN3
CEN9-CEN3
CEN10-CEN3
CEN11-CEN3
CEN12-CEN3
CEN13-CEN3
CEN14-CEN3
CEN15-CEN3
CEN16-CEN3

Figure 8A

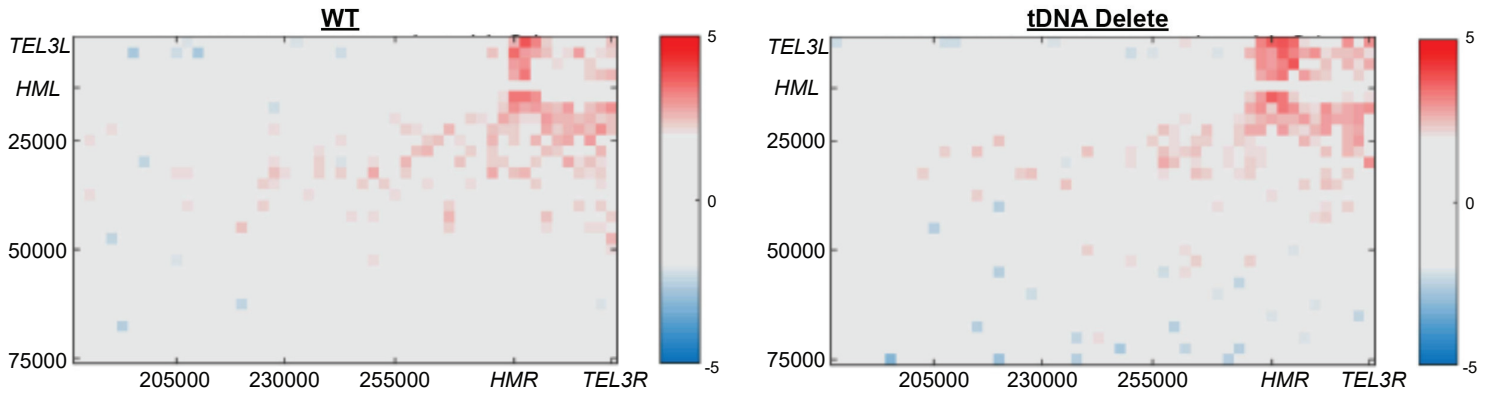

Figure 8B.

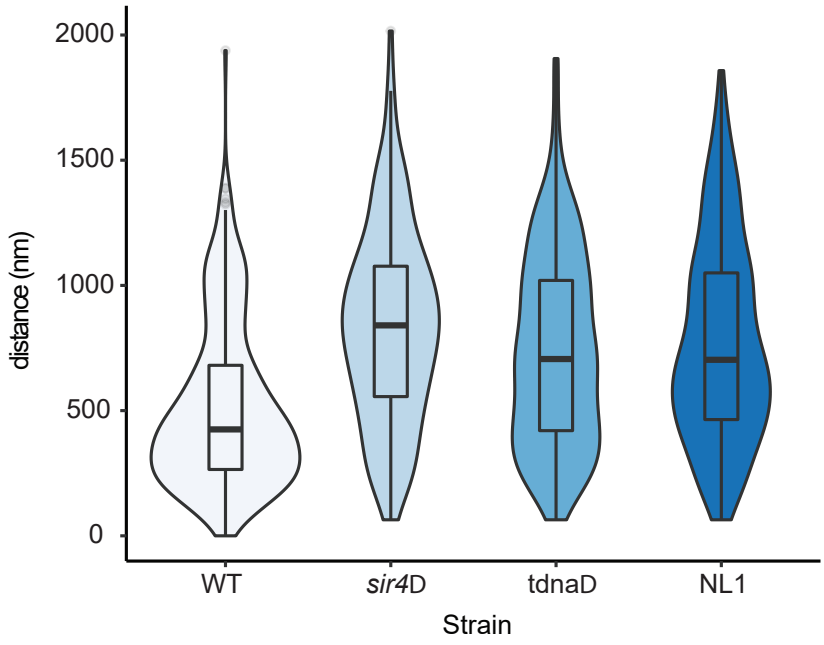

Figure 8C

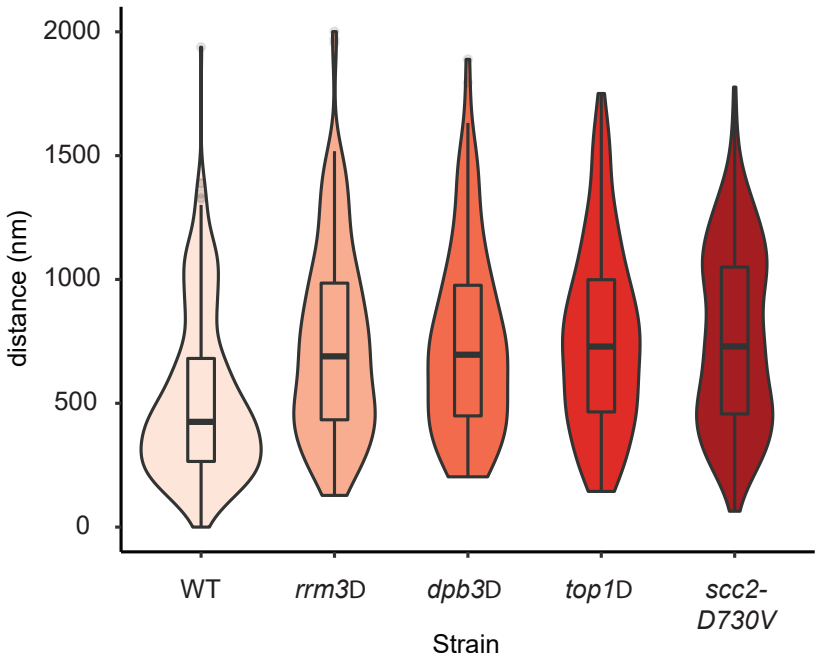

Figure 9A

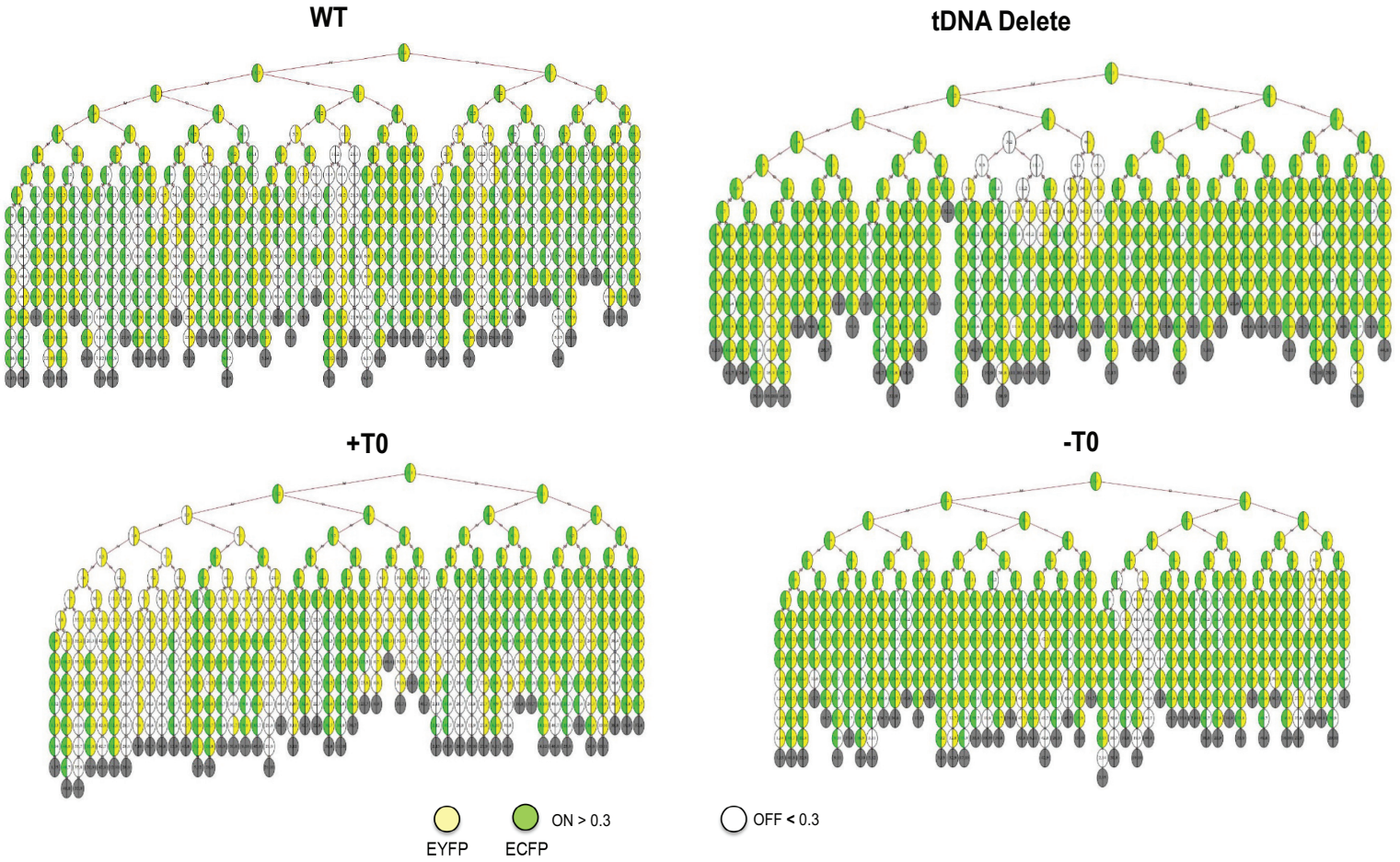

Figure 9B

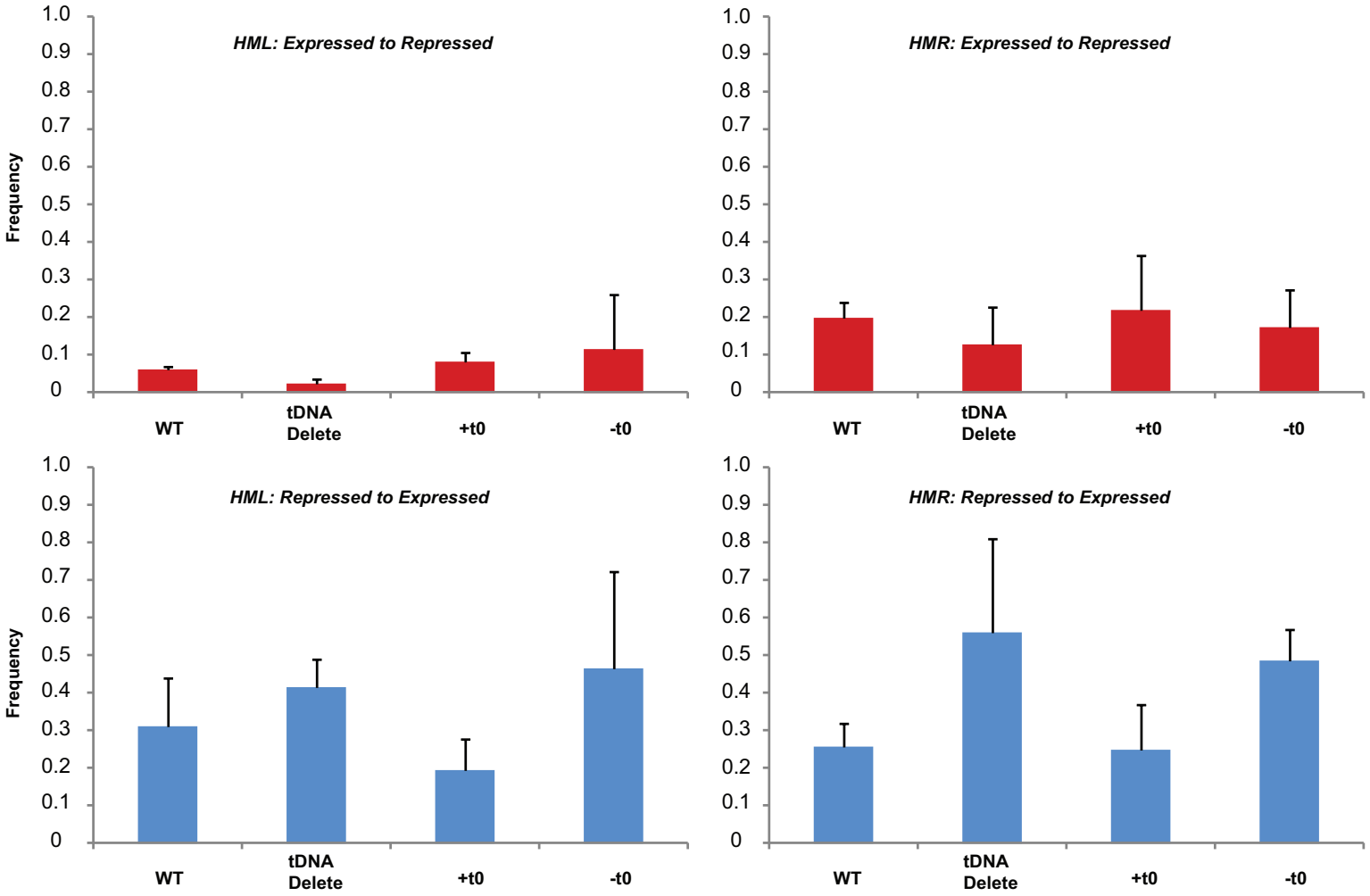

Upregulated in tDNA del	q-Val (likelihood ratio test)	q val (Wald test)	beta statistic	Gene Name	Function
YCR061w	0.042003857	3.22E-11	0.6580998		Protein of unknown function
YDL124w	0.042003857	6.31E-14	0.4395261		NADPH-dependent alpha-keto amide reductase
YHR214c-B	0.005672182	2.35E-210	2.5870238		Retrotransposon TYA Gag and TYB Pol genes
YNL160w	0.040272092	2.69E-20	0.5348964	YGP1	Cell wall-related secretory glycoprotein
YOR201c	0.020396347	9.18E-27	0.7685378	MRM1	Ribose methyltransferase
YOR202w	0.009117145	1.20E-76	3.7326308	HIS3	Imidazoleglycerol-phosphate dehydratase
YPL240c	0.042003857	1.20E-15	0.5188043	HSP82	Hsp90 chaperone

Downregulated	q-Val (likelihood ratio test)	q val (Wald test)	beta statistic		
YBR068c	0.030966243	1.53E-20	-0.5156825	BAP2	High-affinity leucine permease
YBR296c	0.039894621	1.87E-19	-0.5692597	PHO89	Plasma membrane Na+/Pi cotransporter
YCR008w	0.015662463	6.48E-43	-1.1217	SAT4	Ser/Thr protein kinase involved in salt tolerance
YER073w	0.045197971	8.81E-16	-0.5691673	ALD5	Mitochondrial aldehyde dehydrogenase
YER091c	0.042003857	1.79E-20	-0.5345605	MET6	Cobalamin-independent methionine synthase
YGL009c	0.009117145	1.47E-82	-2.0202761	LEU1	Isopropylmalate isomerase
YHR208w	0.007776891	7.72E-106	-1.3235331	BAT1	Mitochondrial branched-chain amino acid (BCAA) aminotransferase
YJR010w	0.042003857	3.34E-13	-0.8073784	MET3	ATP sulfurylase involved in methionine metabolism
YJR016c	0.017736878	3.09E-29	-0.5823368	ILV3	Dihydroxyacid dehydratase involved in biosynthesis of branched chain amino acids
YKL030w	0.042003857	3.46E-11	-0.6718075		Dubious open reading frame
YKL120w	0.007776891	1.47E-94	-1.4546702	OAC1	Mitochondrial inner membrane transporter
YLR355c	0.042003857	2.35E-12	-0.387429	ILV5	Acetohydroxyacid reductoisomerase involved in biosynthesis of branched chain amino acids
YMR108w	0.042003857	3.72E-15	-0.4213145	ILV2	Acetolactate synthase involved in isoleucine and valine biosynthesis
YOR271c	0.027535084	4.63E-26	-0.5903308	FSF1	Putative protein of the sideroblastic-associated protein family

Strain	Genotype Information
JKY562	MATa t0D, t1D, t2D, t3D, t4D, t5D, t6D, t7D, t8D+t9D T1+T7::HIS3 Laci-GFP::ADE2 LEU2 BRN1-HA::KanMx
JKY702	MATa t0D, t1D, t2D, t3D, t4D, t5D, t6D, t7D, t8D+t9D T1+T7::HIS3 Mcd1-13xMyc::KanMx LacI-GFP::ADE2
ROY5151	MATa t0D, t1D, t2D, t3D, t4D, t5D, t6D, t7D, t8D+t9D::LEU2 T1+T7::HIS3 ade2- LYS2+ SCC2-13xMyc::KanMx
ROY4825	MATa HMR(s288c) SCC2-13XMyc::KanMx ADE2 his3 leu2 lys2 trp1 ura3
ROY4925	MATa HMR(s288c) Mcd1-13Xmyc::KanMx ADE2
ROY4927	MATα HMR(s288c) BRN1-HA::KanMx ADE
ROY5750	MATa LacI-GFP::ADE2 lys2- TEL3L::LacO::TRP1 SPC29-RFP::Hyg t0D, t1D, t2D, t3D, t4D, t5D, t6D, t7D, t8D+t9D::LEU2? T1+T7::HIS3
ROY5751	MATa LacI-GFP::ADE2 lys2- TEL3L::LacO::TRP1 SPC29-RFP::Hyg t0D, t1D, t2D, t3D, t4D, t5D, t6D, t7D, t8D+t9D::LEU2? T1+T7::HIS3
ROY5670	LacI-GFP::ADE2 TEL3L::LacO::TRP1 SPC29-RFP::Hyg
ROY5671	LacI-GFP::ADE2 TEL3L::LacO::TRP1 SPC29-RFP::Hyg
ROY5695	LacI-GFP::ADE2 lys2- Chr3L(mid)::LacO::TRP1 SPC29-RFP::Hyg t0D, t1D, t2D, t3D, t4D, t5D, t6D, t7D, t8D+t9D::LEU2 T1+T7::HIS3
ROY5696	LacI-GFP::ADE2 lys2- Chr3L(mid)::LacO::TRP1 SPC29-RFP::Hyg t0D, t1D, t2D, t3D, t4D, t5D, t6D, t7D, t8D+t9D::LEU2 T1+T7::HIS3
ROY5672	LacI-GFP::ADE2 Chr3L(mid)::LacO::TRP1 SPC29-RFP::Hyg
ROY5689	LacI-GFP::ADE2 56xLacO::LEU2 SPC29-RFP::Hyg t0D, t1D, t2D, t3D, t4D, t5D, t6D, t7D, t8D+t9D T1+T7::HIS3
ROY5690	LacI-GFP::ADE2 56xLacO::LEU2 SPC29-RFP::Hyg t0D, t1D, t2D, t3D, t4D, t5D, t6D, t7D, t8D+t9D T1+T7::HIS3
ROY5317	MAT@ LacI-GFP::ADE2 lys- 56xLacO::LEU2 SPC29-RFP::Hyg
ROY5318	MAT@ LacI-GFP::ADE2 lys- 56xLacO::LEU2 SPC29-RFP::Hyg
ROY5290	MAT@ LacI-GFP::ADE2 126xLacO::CEN3::TRP1 spc29-RFP::Hyg t0D, t1D, t2D, t3D, t4D, t5D, t6D, t7D, t8D+t9D T1+T7::HIS3 leu2-
ROY5291	MAT@ LacI-GFP::ADE2 64xLacO::CEN3::TRP1 spc29-RFP::Hyg t0D, t1D, t2D, t3D, t4D, t5D, t6D, t7D, t8D+t9D T1+T7::HIS3 leu2-
ROY5288	MATa LacI-GFP::ADE2 126xLacO::CEN3::TRP1 spc29-RFP::Hyg
ROY5289	MATa LacI-GFP::ADE2 126xLacO::CEN3::TRP1 spc29-RFP::Hyg
ROY5748	MATa LacI-GFP::ADE2 t2::56xLacO::LEU2 SPC29-RFP::Hyg t0D, t1D, t2D, t3D, t4D, t5D, t6D, t7D, t8D+t9D T1+T7::HIS3 leu2-
ROY5749	MATa LacI-GFP::ADE2 t2::56xLacO::LEU2 SPC29-RFP::Hyg t0D, t1D, t2D, t3D, t4D, t5D, t6D, t7D, t8D+t9D T1+T7::HIS3 leu2-
ROY5668	MAT@ LacI-GFP::ADE2 t2wt::56xLacO::LEU2 SPC29-RFP::Hyg
ROY5669	MAT@ LacI-GFP::ADE2 t2wt::56xLacO::LEU2 SPC29-RFP::Hyg
ROY5319	MATa LacI-GFP::ADE2 lys- MAT::LacO::TRP1 SPC29-RFP::Hyg t0D, t1D, t2D, t3D, t4D, t5D, t6D, t7D, t8D+t9D::LEU2 T1+T7::HIS3
ROY5320	MATa LacI-GFP::ADE2 lys- MAT::LacO::TRP1 SPC29-RFP::Hyg t0D, t1D, t2D, t3D, t4D, t5D, t6D, t7D, t8D+t9D::LEU2 T1+T7::HIS3
ROY5294	MAT@ LacI-GFP::ADE2 MAT::LacO::TRP1 lys- SPC29-RFP::Hyg
ROY5359	MAT@ LacI-GFP::ADE2 lys- MAT::LacO::TRP1 SPC29-RFP::Hyg
ROY5687	MATa LacI-GFP::ADE2 t1::56xLacO::LEU2 SPC29-RFP::Hyg t0D, t1D, t2D, t3D, t4D, t5D, t6D, t7D, t8D+t9D T1+T7::HIS3 leu2-
ROY5688	MAT@ LacI-GFP::ADE2 t1::56xLacO::LEU2 SPC29-RFP::Hyg t0D, t1D, t2D, t3D, t4D, t5D, t6D, t7D, t8D+t9D T1+T7::HIS3 leu2-
ROY5666	MAT@ LacI-GFP::ADE2 t1wt::56xLacO::LEU2 SPC29-RFP::Hyg
ROY5667	MAT@ LacI-GFP::ADE2 t1wt::56xLacO::LEU2 SPC29-RFP::Hyg
ROY5321	MAT@ LacI-GFP::ADE2 lys- GIT1::56xLacO::TRP1 SPC29-RFP::Hyg t0D, t1D, t2D, t3D, t4D, t5D, t6D, t7D, t8D+t9D::LEU2 T1+T7::HIS3
ROY5323	MAT@ LacI-GFP::ADE2 lys- GIT1::56xLacO::TRP1 SPC29-RFP::Hyg t0D, t1D, t2D, t3D, t4D, t5D, t6D, t7D, t8D+t9D::LEU2 T1+T7::HIS3
ROY5664	LacI-GFP::ADE2 GIT1::56xLacO::TRP1 SPC29-RFP::Hyg
ROY5665	LacI-GFP::ADE2 GIT1::56xLacO::TRP1 SPC29-RFP::Hyg
JKY689	MATa tDNA0 (WT) t1D, t2D, t3D, t4D, t5D, t6D, t7D, t8D+t9D T1+T7::HIS3 LEU2 ade2-1
ROY1681	MAT@ ADE2 his3 leu2 lys2 trp1 ura3 HMR (t-RNA bound delete)
JKY690	MATa t0D, t1D, t2D, t3D, t4D, t5D, t6D, t7D, t8D+t9D T1+T7::HIS3 LEU2 ade2-1 LYS+
JRY2334	MATa ade2-1 can1-100 his3-11 leu2-3,112 trp1-1 ura3-1 GAL
ROY4830	MATa/MAT@ HML-TetO :: LEU2 HMR-LacO:: TRP1 CFP-LacI-TetR-YFP::ADE2 LYS2
ROY4846	MAT@ LacO(256x)::GIT1::TRP1 HML-TetO::LEU2 CFP-LacI-TetR-YFP::ADE2 tT(AGU)CΔ::URA3 lys2Δ
ROY4859	MAT HML-tetO::LEU2 HMR-LacO::TRP1 CFP-LacI-TetR-YFP::ADE2 sir4Δ::URA3 lys-

ROY4860	MAT HML-tetO::LEU2 HMR-LacO::TRP1 CFP-LacI-TetR-YFP::ADE2 sir4Δ::URA3 lys-
ROY5518	MATa LacI-GFP::ADE2 lys2- Chr3L(mid)::LacO::TRP1 t0D, t1D, t2D, t3D, t4D, t5D, t6D, t7D, t8D+t9D::LEU2 T1+T7::HIS3
ROY5521	MATa lys- LacI-GFP::ADE2 Chr3L(mid)::LacO::TRP1
ROY5602	MATa LacI-GFP::ADE2 56xLacO::LEU2 t0D, t1D, t2D, t3D, t4D, t5D, t6D, t7D, t8D+t9D T1+T7::HIS3
GRY911	MATa LacI-GFP::ADE2 56xLacO::LEU2 lys-
GRY907	MAT@ LacI-GFP::ADE2 56xLacO::LEU2 lys- trp- ura- his-
GRY872	MAT@ 126xLacO::CEN3::TRP1 t0D, t1D, t2D, t3D, t4D, t5D, t6D, t7D, t8D+t9D T1+T7::HIS3 leu2-3, 112 LacI-GFP::ADE2 trp- lys- ura-
GRY823	Mata LacI-GFP::ADE2 LacO(64x)::CEN3::TRP1
GRY824	MAT@ LacI-GFP::ADE2 LacO(64x)::CEN3::TRP1
ROY5512	MATa LacI-GFP::ADE2 t2::56xLacO::LEU2 t0D, t1D, t2D, t3D, t4D, t5D, t6D, t7D, t8D+t9D T1+T7::HIS3 leu2-
ROY5510	MAT@ lys- LacI-GFP::ADE2 t2wt::56xLacO::LEU2
GRY938	MAT@ t1Δ::URA3 t0D, t1D, t2D, t3D, t4D, t5D, t6D, t7D, t8D+t9D::LEU2 T1+T7::HIS3 LacI-GFP::ADE2 HMR-GIT1::TRP1 lys-
GRY883	MAT@ t1WT@HIS3 t1WT::URA3 GIT1::TRP1 LYS+ LEU+ ade-
GRY935	MATa LacI-GFP::ADE2 t0D, t1D, t2D, t3D, t4D, t5D, t6D, t7D, t8D+t9D T1+T7::HIS3 trp- leu- lys- ura-
GRY963	MAT@ t0D, t1D, t2D, t3D, t4D, t5D, t6D, t7D, t8D+t9D T1+T7::HIS3 LYS+ ade- leu-
JRY4012	MATa can1-100 his3-11 leu2-3,112 lys2Δ trp1-1 ura3-1 GAL

Primer Name	Sequence 5'-3'	Amplicon
yOH58	TACTACAAGAGAAAGGCCATCTCC	t1
yOH59	AATGCAGCGCAGACAGCACAGTT	t1
QJK61	TTGAGATACAAAATATTACAAGAAGTCCTG	t2
QJK62	GCGTTCTTCTGTATCTGAAGATAGTG	t2
QJK63	TCATGTATCAAGATTACTAGCGCAAGTG	t5
QJK64	TTCTATTCTTATGTACCGTTCCGCC	t5
yOH62	GCAAGCGAAGTTGTTCCCGTTAT	t7
yOH63	GTTCGGTCACTTAGAGGATATAATTG	t7
QJK69	CTCTATTTCTCAACAAGTAATTGGTTGTTT	t8
QJK70	GCCCCTGTGTGTTCTCGTTATGT	t8
yOH64	GACAAGAAAGATAACGACACAGTGA	t9
yOH65	GGCCCTCGTATAGTCTCTTTTC	t9
R197	GAGACCAGGTTTATTCAACCGGTAAC	t0
LOU120	GGGTGTCACCGAATAACGTGAT	t0
GRO39	TAAGACAATTGTGGACAACAAAGCAAA	*OCA4*
GRO40	ATTTATTAATGTCAAAAGCCGCTGAGG	*OCA4*
yOH66	TCACTCATATAAACCGAACCCTTCC	CEN3
yOH67	GGATTTTCCATATTGTTTGGCGCTG	CEN3

	HMR (Exp to Rep)	HMR (Rep to Exp)	HML (Exp to Rep)	HML (Rep to Exp)
WT	0.2 (0.019)	0.25 (0.031)	0.06 (0.005)	0.3 (0.075)
tDNA Delete	0.13 (0.057)	0.56 (0.145)	0.02 (0.006)	0.41 (0.041)
t0+	0.22 (0.085)	0.25 (0.070)	0.08 (0.014)	0.19 (0.049)
t0-	0.18 (0.049)	(0.48 (0.041)	0.11 (0.072)	0.46 (0.12)